Modulated Phases in Systems with Competing Interactions

A thesis submitted to the
Tata Institute of Fundamental Research, Mumbai 400005
for the degree of
Master of Science in Physics

by
Kazi Rajibul Islam
Department of Theoretical Physics, School of Natural Sciences
Tata Institute of Fundamental Research, Mumbai 400005
July, 2007

I dedicate this humble work to Nanubhai (my grandfather) and to
the fond memory of Nanima (my grandmother).

Declaration

This thesis is mainly a review work. Every effort is made to cite proper references. I have not submitted this work to earn any other degree or course credit.

This work was done under the supervision of Prof. Mustansir Barma, at the Tata Institute of Fundamental Research, Mumbai.

(Kazi Rajibul Islam)

In my capacity as the supervisor of the candidate's thesis, I certify that the above statements are true to the best of my knowledge.

(Prof. Mustansir Barma)
Date:

Acknowledgements

First of all, I would like to express my sincere gratitude to Prof. Mustansir Barma, my thesis advisor. It was a wonderful experience working with him for last one year. His scientific insight and teaching ability are remarkable. I thank him also for the wonderful courses he taught in 2005 Fall and 2007 Spring.

I thank Prof.Deepak Dhar, Dr.Kedar Damle and Dr.Vikram Tripathi for many a helpful discussion on various topics related to Statistical Physics. I also got benefited from the courses they taught.

I am grateful to Prof. Walter Selke of Lehr- und Forschungsgebiet Physik Institut für Theoretische Physik (B), Germany for providing valuable references over e-mail for this work.

I thank Tridib Sadhu for helping me in the Monte Carlo study for Chapter 3. His expertise in Fortran eased my work a lot.

Basudeb Dasgupta has kindly allowed me to use his thesis format. I am grateful to him for making my job easier.

I would like to thank Sayantani Bhattacharya and Sayantan Sharma for discussion on solitons. Arnab Sen helped me a lot to understand many topics over last two years. I thank him also.

I had been fortunate to have Debasish and Jyotirmoy as my classmates for last five years. I remember our happy days together in Jadavpur University and in Mumbai. I thank them for their constant support. I also thank Swastik for being a wonderful roommate.

Other than with the rest of the D-gang: Debasish, Jyoti and Swastik I spent lots of my free time with Paroma, Ipsita*di*, Nachiketa, Swagata and Arjun. It was always a pleasure to have their company. I

am undecided whether to thank or curse Raju and Chaitali for the tempting smell of chicken and fried rice and what not that they offered me for free everyday, as a neighbour! Jokes apart, I must thank them for their enthusiasms in organizing short trips here and there. I thank Subhabrata*da* and Munmun*di* and all my other friends for their company.

The theory students room had been always very lively. I thank all my colleagues for making this place very comfortable to work. Special thanks to Anindya for his constant help in any kind of computer related problem. I thank all the faculty members of the theory group for valuable discussions. Bathija, Pawar, Girish, Ajay and Shinde had been always very helpful in official matters. I thank all of them.

I take this opportunity to thank all my classmates for creating a nice academic environment. I would like to thank all the active members of Amateur Music Association for organizing so many successful concerts on Indian classical music. I think their effort has enriched the quality of the campus life.

I never liked East Canteen food. Hence I must thank Gopal*da* for delivering Bengali style food to the Hostel for a long time.

I would like to thank all the staff members of TIFR, especially the gardeners for their wonderful job.

Last but not the least, I thank my parents, brothers and all members of my family for their support and inspiration.

Rajibul

Synopsis

There exist condensed matter systems with competing interactions which show very interesting and rich phase diagrams. Examples are provided by periodic arrangements like spin density waves, charge density waves, periodic arrangement of atoms on a crystalline substrate etc. When the periodicity of the modulated structure is a (simple) rational multiple of the underlying lattice vector the system is said to be in a commensurate phase and when it is not so, the system is in an incommensurate phase.

In this thesis we review various aspects of three systems where competing interactions lead to various commensurate and incommensurate phases and transition between them. Our first example is Frank and Van der Merwe model which idealize rare-gas monolayers adsorbed on a host lattice (such as Krypton on graphite) in one dimension. In this model point masses connected by identical springs are subject to an external periodic potential, the misfit between the period of the potential and the natural length of the springs or the strength of the potential relative to the spring constant being the parameters to be tuned. This model shows commensurate-incommensurate phase transitions as these parameters are varied, a consequence of the competition between the elastic and the potential energy.

The next example is the Axial Next Nearest Neighbour Ising (ANNNI) Model. In this model spin-$\frac{1}{2}$ objects reside on a cubic lattice and along one axis (say z-axis) interact with nearest neighbours via a ferromagnetic exchange coupling ($J_1 > 0$) and with next nearest neighbours via an antiferromagnetic exchange coupling ($J_2 < 0$). In the plane perpendicular to this axis, the spins interact ferromagnetically with nearest neighbours. The ground state of this system depends on the ratio of the couplings. In fact, at $\frac{|J_2|}{J_1} = \frac{1}{2}$ the ground state is not unique like many other frustrated systems and there is an infinity of degenerate ground states

in the thermodynamic limit (the degeneracy increases exponentially with the system size). This point is known as multiphase point. For $\frac{|J_2|}{J_1} < \frac{1}{2}$ the ground state is ferromagnetic and for $\frac{|J_2|}{J_1} > \frac{1}{2}$ it has up-up-down-down spin structure (known as (2,2) antiphase) along the axis, all the spins in the planes perpendicular to this axis being aligned in the same direction in the absence of competing interactions within a plane.

At low but non-zero temperatures, this model shows an infinite sequence of phases of the sort $< 2^{j-1}3 >$ ($j = 1, 2, \ldots$; for example $< 2^3 3 >= \ldots \uparrow\uparrow\downarrow\downarrow\uparrow\uparrow\downarrow\downarrow\downarrow \ldots$, the sequence represents majority spins at successive planes perpendicular to the z-axis) between the ferromagnetic and the (2,2) antiphase. All these phases spring out from the multiphase point. At higher temperatures various other commensurate and incommensurate spatially modulated phases are obtained.

In this model the transitions between the ferromagnetic and other spatially modulated phases are first order in nature, all the way from the multiphase point up to the Lifshitz point, a special type of tricritical point at which ferromagnetic phase coexists with paramagnetic and spatially modulated phase.

The next example of systems with competing interactions is real closed packed materials like SiC, ZnS etc that show variable periodicity along some crystallographic axis, a phenomenon known as polytypism. Atomic layers can be stacked in many ways along this axis like ...ABCABC... or ...ABABAB... or ...ABCACB... or any other sequence where same letters do not sit next to each other and hence variable periodicity is observed. The letters A,B,C represent three possible relative positions for atoms in closed packed structure. Polytypism refers to different structures of this type observed in crystals of same material. Transition from one polytype structure to another is obtained as temperature, pressure or chemical environment is varied.

The similarity between the sequence of phases in polytypes and the ANNNI model motivates to cast the polytype problem to ANNNI model, extended to include the third nearest neighbour interaction. Between successive layers in the polytype, spin variables are introduced: spin 'up' if the letters A,B,C occur cyclically and spin 'down' otherwise. Next we look at a plausible dynamics of transformation and its consequences, from one polytypic structure (3C phase, ...AB-

CABC..., in spin language all 'up' phase) to another (6H phase, ...ABCACB..., in spin language ... $\uparrow\uparrow\uparrow\downarrow\downarrow\downarrow$ ...). In spin language the dynamics turns out to be trimer flip under energetically favourable conditions. Using a Monte Carlo simulation at $T = 0$ we looked at the system when it was quenched to 6H phase suddenly. If the initial configuration was all 'up-spins' (3C phase) it turned out that the system got stuck at some intermediate 'metastable states'. If quenched to the 3C-6H phase boundary, the spins remain active for a large number of Monte Carlo steps. With a random initial configuration the final state was found to be different. The system showed 'active' and 'frozen' spin patches when quenched to 3C-6H phase boundary. Thus the final state reached through this dynamics is dependent on the initial condition.

Contents

Chapter 1

Introduction

Systems under the influence of competing 'forces' often show very interesting phenomena. Simple examples are provided by oscillatory systems, like a pendulum or a spring-mass system. The competing 'forces' might be gravity and elastic forces as in case of a spring-mass system hanging from a point or might be the 'Pauli degeneracy pressure' and gravity as in the case of neutron stars on the verge of collapsing into a black hole. There are also condensed matter systems where competing interactions lead to interesting properties.

In this thesis, we shall try to look at a few examples where this is the case. The first example will be a very simple model originally introduced by Frenkel and Kontorowa but later studied by many authors, notably by Frank and Van der Merwe and some others. The model is known as Frank and Van der Merwe (FVdM) model and involves one dimensional array of masses connected by springs and subject to an external periodic potential. This might be thought of an idealized one dimensional model for rare-gas monolayer adsorbed on graphite surface. The periodic potential is due to the underlying graphite lattice. Competition between the elastic energy of the springs and the potential energy lead to interesting properties of the system.

The second example is a simple Statistical Physics model, known as Axial Next Nearest Neighbour Ising (ANNNI) model where scalar spins sitting on a hypercubic lattice interact with nearest neighbours via ferromagnetic exchange coupling and with next nearest neighbours via antiferromagnetic exchange coupling along one axis. In the plane perpendicular to the axis, the spins interact

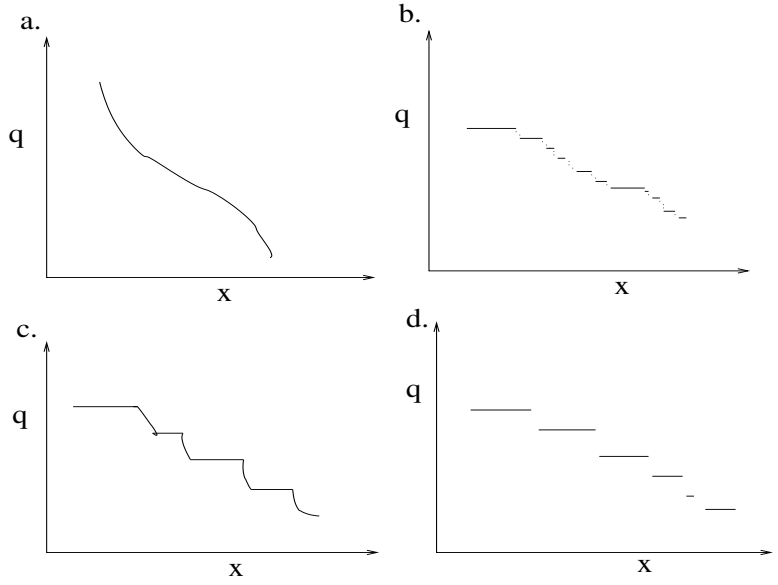

Figure 1.1: Various possible cases of variation of ordering wave vector q (the inverse period) with external tuning parameter x. (a) Smooth analytic behaviour. (b) Complete devil's staircase. (c) Incomplete Devil's staircase. (d) Harmless Devil's Staircase.

ferromagnetically with nearest neighbours. Hence this model involves competing interactions along one axis.

The last example will be provided by an interesting phenomenon called 'Polytypism' seen in some crystalline matter, the classic examples being SiC, ZnS etc. These materials have closed packed structures and along some crystallographic axis they show variable periodicity in their lattice structure.

In this chapter, we shall introduce various concepts and terms relevant to systems with competing interactions. They will be made precise later when we come to concrete examples in the later chapters.

Commensurate Phases: A modulated phase is said to be commensurate when the period of the ordered phase is a (simple) commensurate multiple of the underlying lattice periodicity.

Incommensurate Phases: When the period of the ordered phase is incommensurate with the underlying lattice periodicity the phase is known as an in-

commensurate phase.

Devil's Staircase: As some external parameter (say x, it might be temperature, pressure etc) is varied the ordering wave vector (say q) might change in various possible ways as follows:
(a) q might change continuously as x is varied.
(b) q might lock at an infinity of commensurate values. In the case where locking happens $q - x$ curve looks like a staircase and hence the picturesque name 'Devil's Staircase' is given to it. There might be incommensurate phases between commensurate phases. Then the Devil's staircase is said to be incomplete.[1]
(c) The locked values, taking all possible commensurate numbers, fill up the whole of the argument of x. There are no jumps of first order transition. This case is known as a complete Devil's staircase.
(d) q jumps between commensurate values for some range of x and changes continuously for some other range.
(e) q takes only one of a finite number of rational values as x is varied. This is known as a harmless Devil's staircase. Fig (1.1) shows various cases of Devil's staircase.
Commensurate Incommensurate Transition: The transition from the commensurate to incommensurate structures are understood in terms of a soliton theory[[2],[3]]. Within this framework 'solitonic walls' represent spatially incommensurate regions between commensurate regions. If at some temperature the formation energy of 'solitonic walls' becomes negative, the commensurate phase will be unstable against an incommensurate phase. In chapter 2 where we have discussed FVdM model in somewhat more detail, this point is elaborated.
ANNNI Model Phase Diagram: Various commensurate and incommensurate phases are obtained in the phase diagram of ANNNI model, topic of our discussion in chapter 3. In this model the crucial parameter is the ratio of the couplings, $\kappa = -\frac{J_2}{J_1}$, J_1 and J_2 being the nearest neighbour ferromagnetic and next nearest neighbour antiferromagnetic coupling respectively. Section (3.2) gives an overview of the phase diagram before we discuss various parts of it in detail in the remaining of the chapter 3. The ground state is ferromagnetic for $\kappa \leq \frac{1}{2}$ and 'up-up-down-down' ($\uparrow\uparrow\downarrow\downarrow$) along z-axis for $\kappa > \frac{1}{2}$. All the

spins in the perpendicular plane is aligned in the same direction in the ground state. The point ($\kappa = \frac{1}{2}, T = 0$) is a multiphase point where the degeneracy of ground states is exponential in system size. From this point phases of the form ($< 2^{j-1}3 >,\ j = 1, 2, ...; < 2^3 3 >= ...\ \uparrow\uparrow\downarrow\downarrow\uparrow\uparrow\downarrow\downarrow$ ...for example) spring out at finite temperatures., as found by Fisher and Selke [[4],[5]]. At higher temperature, various other commensurate phases and incommensurate phases are obtained before the system goes to a paramagnetic phase. The phase diagram has a Lifshitz point where the paramagnetic phase and a uniformly ordered ferromagnetic phase coexist with spatially modulated phases. The complete phase diagram is shown in fig (3.3).

It is interesting to note that long range interaction is not necessarily needed to explain the existence of very long period (or small wave vector) phases. ANNNI model involves short range interactions and still it does show these kinds of phases. ***Polytypes***: Real materials like SiC,ZnS show very interesting phase diagrams. These materials have closed packed structures where the smaller atoms sit in the voids formed by the closed packing of larger atoms. These materials show variable lattice periodicity along the direction of growth. This can be understood in the following way. For a 2-dimensional layer of closed packed spheres (let us name this as A layer) the next layer on top of it can be stacked in two ways. These two positions correspond to centre of the spheres lying on up-void triangles ($\triangle$,call this position B) and on down-void triangles ($\bigtriangledown$, call this position C). Similarly for a B layer the next two possibilities are either A or C. The condition of closed packing (*'Polytypic constraint'*) is that in the packing sequence no two same letters are next to each other. Hence the sequence might be (...ABABAB...), (... ABCABC ...) or (... ABCACB ...) or any other sequence in which no two same letter appear next to each other. In the above cases the periodicities are 2, 3 and 6 lattice spacings and the phases are 2H, 3C and 6H respectively (C refers to the cubic symmetry and H refers to the hexagonal symmetry). Since there is an infinite number of ways one can write down sequences, there can be infinite possible periodicity along the stacking direction. This phenomenon is known as 'Polytypism' and is discussed in Chapter 3. The crystal can undergo phase transitions from one polytypic structure to another when external parameters like

pressure and temperature are changed. There are various theories available to describe the transitions[6].

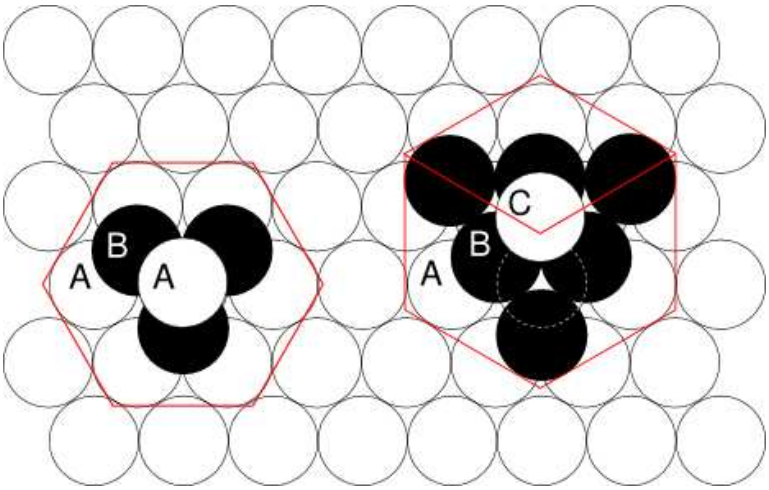

Figure 1.2: The three positions A,B,C in closed packing are shown. At the left hexagonal closed packing (2H) and at the right cubic closed packing (3C) are shown. This figure is taken from Wikipedia. (http://en.wikipedia.org/wiki/Image:Close_packing.png)

.

We have seen that the ANNNI model shows various spatially modulated phases. Now, since there are binary options available for the closed pack stacking at every stage, this problem can be mapped to ANNNI model, in fact an extended ANNNI model which includes third nearest neighbour interaction (the coupling is J_3) also [7]. The similarity of the sequence of phases found in ANNNI model with polytypes provides a motivation for this mapping [8]. Ising variables are assigned on each bond along the growth direction. $S = 1$ if the letters A,B,C appear in cyclic sequence (A$\rightarrow$ B or B$\rightarrow$ C or C$\rightarrow$ A) and $S = -1$ if they appear anti-cyclically, e.g.,(. . . ABC. . .)$\Rightarrow$(. . . $\uparrow\uparrow\uparrow$ . . .), (. . . ABCACB. . .)$\Rightarrow$(...$\uparrow\uparrow\uparrow\downarrow\downarrow\downarrow$...). ***Dynamics of Transformation from one Polytype to another***: We are interested in understanding the dynamics of transitions. Now we need to be very careful while casting the polytype problem in the spin language, for a local move in the spin language might represent moves that are unfavourable in the original problem.

Hence we pick up a particular transition (3C→6H) and identify the local moves in spin language. In this particular case, it turns out to be flipping of 'trimers'- three successive 'up' spins or 'down' spins when the flip is energetically favourable. We do a Monte Carlo study at zero temperature to simulate the dynamics. The system is quenched to $T = 0$ from an initial random or ferromagnetic state. We find that the system might go to a locked state before going to the actual thermodynamically stable phase. A 'locked' phase is a metastable state and is at the local minimum of energy. The true thermodynamically stable phase is at the global minimum of energy and hence once the system gets stuck at the local minimum it has to cross an activation barrier in order to go to states lower in energy, in particular to the thermodynamically stable state. At finite temperatures the system can cross the activation energy barrier to go to other states but the time taken to cross the barrier is exponentially large in the barrier height. Interestingly, on the 3C-6H phase boundary the system shows 'active' and 'locked' patches of spins even after lots of Monte Carlo time steps.

An attempt had been made (Cheng, Needs and Heine [8]) to calculate the couplings J_1, J_2 andJ_3 from band structure calculations of various polytypes, especially SiC. The calculation shows that $J_1 > 0, J_2 < 0$ and$J_3 < 0$ but small. Moreover $-\frac{J_2}{J_1} = \kappa \simeq \frac{1}{2}$. Also the free energy of various polytypes were found to be very close to each other. This shows that the real material is close to the degeneracy point in the ANNNI phase diagram and therefore capable of displaying a large variety of phases, as seen in real polytypes. This is another motivation for studying the Monte Carlo at $T = 0$. However, the absolute value quoted in this calculation seems to be unrealistically low ($J_1 = 0.00485 \pm 0.00120$ eV, $J_2 = -0.00256 \pm 0.00032$ eV and $J_3 = -0.00050 \pm 0.00023$ eV) for real polytypes. We adopt a phenomenological point of view in taking the analogy of ANNNI model with real polytypes. Also, it is an interesting theoretical problem, if not fully realistic, to apply this model to get an insight into plausible dynamics of transformation.

This is mainly a review work. There are lots of papers and articles available on these topics. It was not possible to look at every article. An effort has been made to understand the already established results. In chapter 3 the Monte Carlo programme gives an opportunity to study various questions not previously

studied carefully. Dynamics of polytypic transitions between other phases like 6H-4H are interesting to explore. One needs to find plausible local moves for transitions and then use Monte Carlo code to look at the dynamics.

Chapter 2

The One Dimensional Frank and Van der Merwe Model

The model we are going to discuss in this chapter is probably the simplest model involving competing interactions. Though this model was first proposed by Frenkel and Kontorowa (1938) [9], it was extensively studied by several authors like Frank and Van der Merwe (1949) [10], Theodorou and Rice (1978) [11], Aubry (1979) [1] etc and in the literature this model is referred to as Frank and Van der Merwe (FVdM) model [2].

2.1 The FVdM Model and its Hamiltonian

Our system is a one dimensional array of point masses connected with springs. All the springs are identical and have natural lengths a_0. The masses are subject to an external periodic force with periodicity b. The system is shown in fig (2.1). The Hamiltonian might be taken as,

$$\mathcal{H} = \sum_n \frac{1}{2}k\left(x_{n+1} - x_n - a_0\right)^2 + V\left(1 - \cos\frac{2\pi}{b}x_n\right). \tag{2.1}$$

Here the n^{th} mass has coordinate x_n, k is the spring constant (all the springs are assumed to be identical) and V is the strength of the potential. Let us first note that the first term in (2.1), the elastic energy term will favour all the masses separated by the natural length of the springs, a_0. But the second

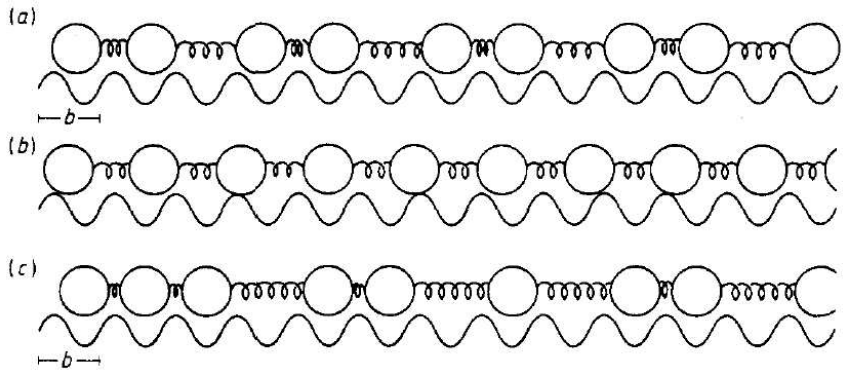

Figure 2.1: The masses connected by springs and subject to an external potential (shown by the wavy line).(a) Commensurate structure,(b) Incommensurate structure and (c) Chaotic structure. (taken from ref[2])

term, the potential energy term will favour the masses to sit at the minima of the potential, i.e., separated by integer multiples of b. These two quantities, namely a_0 and b are in general different and their ratio might be irrational or incommensurate also. The ground state of the problem will be dictated by these two competing terms and might be a commensurate phase, an incommensurate phase or a chaotic phase. In case of a commensurate phase the average separation between the masses will bear a simple ratio with the period of the potential. In an incommensurate phase the average distance between masses is incommensurate to the period of the potential. Apart from these two phases there might be a third type of phase where the potential is strong enough for the masses to sit at the minima. This has been referred to as a 'chaotic' phase[2].

2.2 Minimization of the Energy: Sine Gordon Equation

If we make a change of variable in (2.1)

$$x_n = nb + \frac{b}{2\pi}\phi_n, \tag{2.2}$$

and then take the continuum limit, (2.1) reduces to the following form

$$\mathcal{H} = \int \left(\frac{1}{2} \left(\frac{d\phi}{dn} - \delta \right)^2 + V(1 - \cos\phi) \right) dn \tag{2.3}$$

where k and other constants have been absorbed in $\mathcal{H}$ and V and $\delta = \frac{2\pi}{b}(a_0 - b)$.

The minimization condition of ((2.1) is given by the Sine-Gordon equation,

$$\frac{d^2\phi}{dn^2} - V \sin\phi = 0 \tag{2.4}$$

Since (2.4) is an ordinary second order differential equation, we need two constants. Upon first integration of (2.4) we get,

$$\dot{\phi}^2 = -2V \cos\phi + c_1. \tag{2.5}$$

Here c_1 is an integration constant. Hence, integrating again, we get

$$\int \frac{d\phi}{\sqrt{c_1 - 2V\cos\phi}} = \int dn + c_2 \tag{2.6}$$

The integration constant c_2 is arbitrary since (2.4) is translationally invariant along n. If we choose $c_1 = 2V$ the solution of (2.4) is a single soliton,

$$\phi = 4 \arctan\ \exp\left(n\sqrt{V}\right). \tag{2.7}$$

For $n \to -\infty$, $\phi = 0$ and for $n \to \infty$, $\phi = 2\pi$. The solution looks like as shown in fig (2.2), ϕ has changed from 0 to 2π within a region of width $\frac{1}{\sqrt{V}}$.

For general values of c_1, the solution comes in terms of Elliptic functions. The function looks like what is shown in fig (2.3). There are soliton like walls separating spatially commensurate regions. Within a 'wall' the system is incommensurate. This regular arrangement of soliton like walls is known as a 'solitonic lattice'.

Now, the average misfit between the chain and the lattice, $\bar{q} = \frac{2\pi}{b}(a - b)$ is given by,

$$\bar{q} = \frac{2\pi}{l} \tag{2.8}$$

where l is the distance between the solitons. Since $\bar{q}$ is inversely proportional to the distance between the solitonic walls it can be thought of as the soliton density.

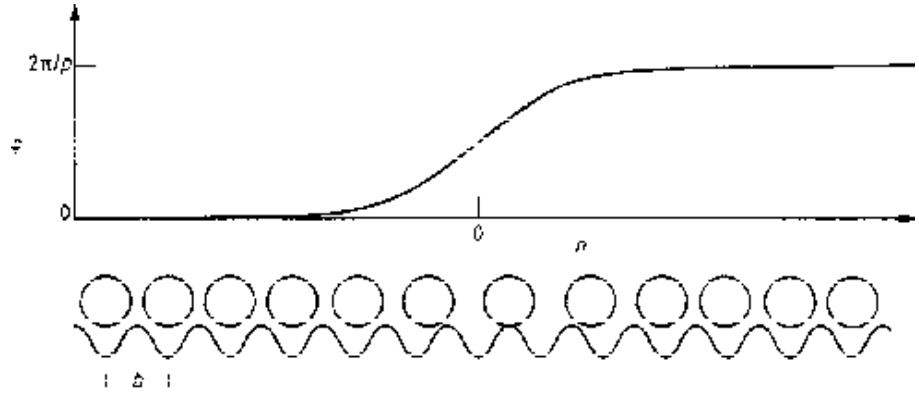

Figure 2.2: A single solitonic solution for $\phi(n).p = 1$ here. The position of the masses are shown. The soliton spatially separates two commensurate regions. (taken from ref[2])

Near the commensurate phase when the soliton density is low, the energy density takes the form [12],

$$E = \left(\frac{4\sqrt{V}}{\pi} - \delta\right)\bar{q} + \frac{16\sqrt{V}}{\pi}\bar{q}\ \exp\left(-\frac{2\pi\sqrt{V}}{\bar{q}}\right). \tag{2.9}$$

Since the first term in (2.9) is proportional to the soliton density, it can be thought of as soliton formation energy and the second term might be thought of as weak repulsion between the solitons.

2.3 Transition to Incommensurate Structure

We see that for sufficient large δ and small V the formation energy becomes negative. Then soliton formation is energetically favourable and the system goes to an incommensurate phase.

Hence the critical value of the potential V at the commensurate-incommensurate transition is

$$V_c = \frac{\pi^2\delta^2}{16}. \tag{2.10}$$

If the potential is weaker than this critical value, the 'elastic energy' of the springs wins in its competition with the potential energy.

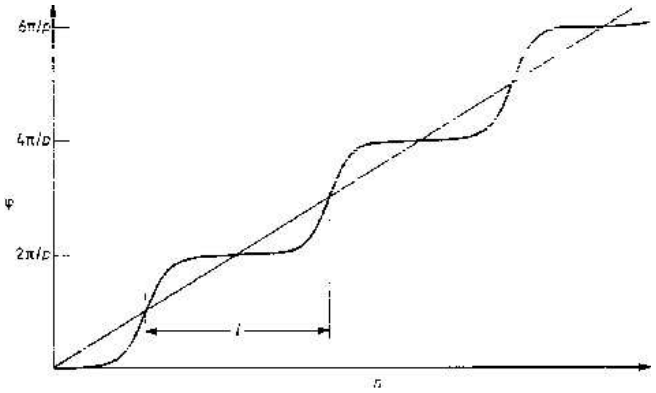

Figure 2.3: Regular solitonic lattice solution for $\phi(n)$ $(p = 1)$.The straight line shows the unperturbed line that corresponds to an incommensurate phase.(taken from ref[2])

Hence this simple model has a phase transition from commensurate to incommensurate phase. We shall come across this Hamiltonian again in the next chapter. The free energy functional in ANNNI model near some commensurate phases can be cast, with proper variable substitution, into this form. That will help us understand the commensurate-incommensurate transition in ANNNI model in the same way.

Conclusion: Experimentally much attention has been paid to commensurate to incommensurate transition in krypton adsorbed on graphite lattice (see ref [13] and references there in). Even though FVdM model is very idealized, it does show commensurate-incommensurate transition. In reality, the adsorbed atoms will also distort the potential. FVdM model needs to be modified to capture this aspect.

Chapter 3

The Axial Next Nearest Neighbour Ising (ANNNI) Model

The Axial Next Nearest Neighbour Ising (ANNNI) model is one of the simplest spin models involving competing interactions. In spite of the simplicity of the model, it does show a very rich and interesting phase diagram. The three dimensional version of this model was first introduced by Elliot [14]. Fisher and Selke first gave the name 'ANNNI model' to it [4]. In the following we shall first define the model and then look at the various possible phases that the model supports.

3.1 Description of the Model

On a d-dimensional hypercubic lattice scalar spins $S = \pm 1$ reside on each site. (We shall often denote $S = 1$ state as $\uparrow$ and $S = -1$ as $\downarrow$.)Each spin interacts with nearest neighbour and next nearest neighbour spins along one axis, say $z-$axis, the exchange couplings being J_1 and J_2, and with all other spins in the hyperplane perpendicular to $z-$axis by a strong ferromagnetic exchange coupling J_0. The Hamiltonian is given by

$$H = -J_0 \sum_{<ij>,z} S_{iz}S_{jz} - J_1 \sum_{iz} S_{iz}S_{iz\pm 1} - J_2 \sum_{iz} S_{iz}S_{iz\pm 2}, \tag{3.1}$$

where indices i and j refer to coordinates (sites) in the $(d-1)$ dimensional hyperplane and angular bracket in $< ij >$ means nearest neighbour interaction.

We shall be using periodic boundary conditions. In order to have ferromagnetic coupling in $(d-1)$ dimensional hyperplane perpendicular to $z-$axis we choose $J_0 > 0$. We assume that the magnitude of J_0 is large enough and we may neglect any major fluctuation in spins within a hyperplane. Various exchange interactions (J_{ij}) are shown in fig (3.1).

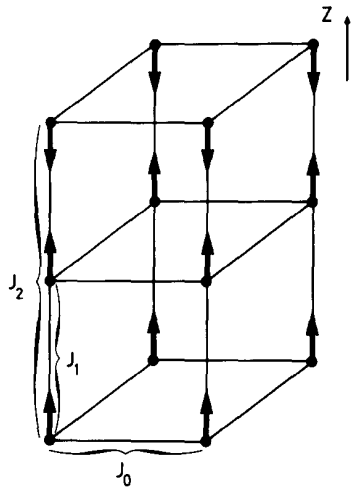

Figure 3.1: The exchange couplings in the Hamiltonian (3.1). (taken from ref[15])

The phase diagram of the model will depend on the signs of J_1 and J_2. In the $(d-1)$ dimensional hyperplane, there are only ferromagnetic interactions unlike along $z-$axis where there might be competing interactions between nearest and next neighbouring spins. Hence we can assume the spins to be oriented along the same direction within a hyperplane and focus on finding out various spin configurations along the $z-$axis. Clearly four options are possible:

A. $J_1 > 0$ and $J_2 > 0 \Rightarrow$ The ground state is ferromagnetic for all values of J_1 and J_2 .

B. $J_1 < 0$ and $J_2 > 0 \Rightarrow$ The ground state is antiferromagnetic for all values of J_1 and J_2.

C. $J_1 > 0$ and $J_2 < 0 \Rightarrow$ The ground state depends on the relative values of the couplings. The system shows frustration as all bonds cannot be satisfied simultaneously. $J_1 > 0$ will prefer an all up (or all down) ground state (...↑↑↑↑...) where as $J_2 < 0$ will prefer up-up-down-down phase (...↑↑↓↓...) as the ground

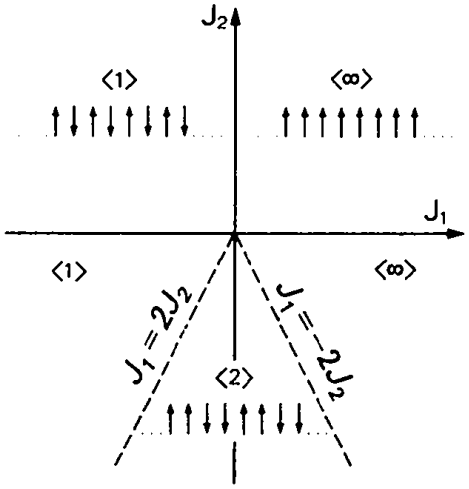

Figure 3.2: The phases at T=0 in the $J_1 - J_2$ plane. There is a huge degeneracy of ground states on the dotted lines, the degeneracy being exponential in system size as will be calculated later [section (3.3.1)]. (taken from ref[15])

.

state. Hence the ground state will depend on the ratio of these two couplings. Since this ratio recurs often, let us reserve a symbol for it. Let $\kappa = -\frac{J_2}{J_1}$.

D. $J_1 < 0$ and $J_2 < 0 \Rightarrow$ The system is frustrated as before. $J_1 < 0$ will prefer a up-down-up-down phase (...↑↓↑↓...) while $J_2 < 0$ will prefer up-up-down-down phase (...↑↑↓↓...) as the ground state. Hance the ground state depends on κ.

The last two cases are examples of what are known as frustrated spin systems. Another famous example of frustrated spin system is the antiferromagnetic nearest neighbour Ising model on a triangular lattice. (See Moessner 2001,[16] and reference therein.) The ground states in cases C and D ($T = 0$) are shown in Figure 3.2. From now on, we shall be working with the case C i.e. $J_1 > 0$ and $J_2 < 0$.

Hence, the model we are interested in is *Axial Next Nearest Neighbour Ising model with nearest neighbour ferromagnetic and next nearest neighbour antiferromagnetic exchange interaction.*

3.2 Overview of the Phase Diagram of the Model

Before going into a detailed analysis of the model, let us discuss the main features of the phase diagram to gain an overview. We shall explain most of the statements and derive most of the results presented here in later sections.

The phase diagram depends on the dimensionality of the lattice. Here we shall be discussing 3 lattice dimensions and briefly mention the properties of phase diagram in 1 and 2 dimensions at the end of this chapter. Since the in-plane coupling, J_0 is ferromagnetic, it is reasonable to consider the spatial modulation along $z-$axis only. We represent various ground state spin configurations of the 3 dimensional system as a chain of spins along $z-$axis. For example,$\uparrow\uparrow\downarrow$ ... will mean that *all* the spins in the first plane are 'up' spins, *all* in the second plane are 'up' spins and *all* in the third plane are 'down' spins and so on. At non-zero temperatures also this notation can be used as long as the in-layer magnetization is non-zero.

Ground State and Low Temperature Phases: At zero temperature there is a first order phase transition from ferromagnetic (...$\uparrow\uparrow\uparrow\uparrow$...) to 'up-up-down-down' phase (...$\uparrow\uparrow\downarrow\downarrow$..., known as Antiphase) at $\kappa = \frac{1}{2}$.

The point $(\kappa = \frac{1}{2}, T = 0)$ is a multiphase point where there is a large degeneracy ($\sim \mu^L$, μ is the golden ratio, $\frac{\sqrt{5}+1}{2} \simeq 1.618...$ and L is the system size, see section (3.3.1)) of ground states. At this point, any spin configuration formed by successive patches of alternate spins of size greater than one is a ground state. At non zero temperatures various phases spring out from this multiphase point. At low temperatures, there is an infinite number of phases between the ferromagnetic and antiphase states. The phases are characterized by spin configurations $< 2^{j-1}3 >$, $j = 1, 2, 3, ...$ (e.g., $< 2^3 3 >= ...\ \uparrow\uparrow\downarrow\downarrow\uparrow\uparrow\downarrow\downarrow\downarrow\ ...$) with wave vectors $\pi j/(2j+1)$ [5]. The transition between various phases are first order in nature and the extent of the phases decrease exponentially as j increases(see section (3.3.2)). At $j \to \infty$ the antiphase state is obtained which is stable over a large $T - \kappa$ region.

High Temperature Phases: Mean Field Theory: At sufficiently high temperatures a paramagnetic phase is found for finite value of κ. As the temperature is lowered the system goes either to a ferromagnetic or to a spatially modulated

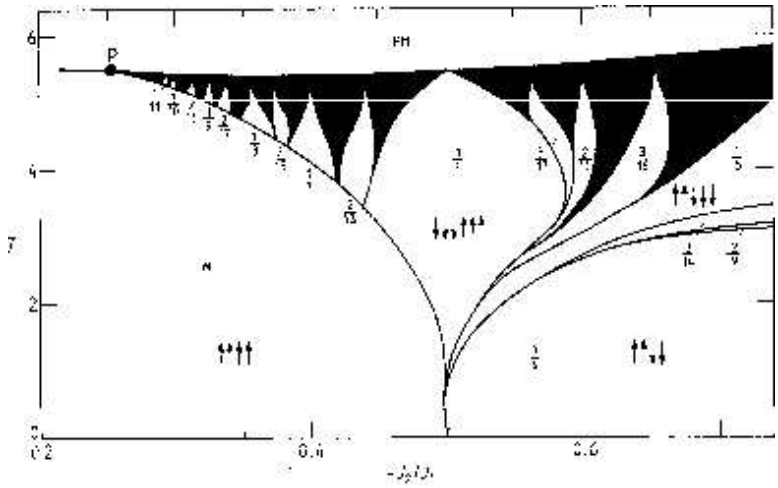

Figure 3.3: The complete phase diagram of the ANNNI model. For simplicity J_0 is taken to be equal to J_1. The black and white stripped region consists of various commensurate phases stable over small $T-\kappa$ range and incommensurate phases. The diagram is taken from ref [3].

phase depending on the value of κ. Within mean field theory, the ferromagnetic phase is obtained for $\kappa \leq \frac{1}{4}$ and spatially modulated phase for $\kappa > \frac{1}{4}$. Both the transitions are of second order in nature. While the transition to the ferromagnetic phase falls in the Ising universality class, those to various modulated phases fall in the $X-Y$ universality class [17]. An exception is provided for $\frac{1}{\kappa} = 0$ ($\kappa \to \infty$) where the 'antiphase' state meets the paramagnetic-modulated phase transition line and the transition again becomes that of Ising universality class as the model breaks into two decoupled Ising models on two independent sublattices. This point is known as 'Decoupling point' and the scaling properties near this point have been studied by Huse and Fisher [18]. The wave vector of spatially modulated phase at the transition temperature,within mean field theory, is given by,

$$2\pi q_c = \arccos \frac{1}{4\kappa} \tag{3.2}$$

where we have set the lattice spacing along $z-$axis to unity. We shall stick to this convention in our entire discussion.

It is interesting to note that according to (3.2) the wave vector might be an

irrational number also, showing transition to a phase that is incommensurate with the underlying lattice periodicity.

The point ($\kappa = \frac{1}{4}, T = 5.5J_1$, the co-ordinate is calculated using mean field theory) is a special type of triple point since here a uniformly ordered phase coexists with paramagnetic and spatially modulated phase. This point is known as Lifshitz Point. The first order transition line from ferromagnetic to modulated phases meets with the second order transition line from the paramagnetic to modulated phase at Lifshitz point. So at this point the jump in the value of magnetization vanishes as one crosses ferromagnetic-modulated phase boundary.

Among the modulated phases, $q = \frac{1}{4}$ and $q = \frac{1}{6}$ phases are stable over a larger area in the phase diagram compared to other phases. The stability of these phases can be understood within a soliton picture where solitonic walls separate commensurate regions spatially (see section (3.4.3)). The positive energy of solitonic wall formation for these two phases over large temperature and κ ranges guarantee the stability of these phases. In the following we try to understand the features of the phase diagram in detail.

3.3 Ground State of the Model and Low Temperature Phase Diagram

The ground state of the model can be solved exactly by looking at energies of various spin configurations as a function of κ. The non-zero but low temperature phase diagram can be obtained using low temperature expansion technique.

3.3.1 Ground State: $T = 0$ phase diagram

For $\kappa = 0$, the model is simply an Ising model with nearest neighbour ferromagnetic interaction, hence the ground state is all 'up' (or all 'down' since there is no external magnetic field) configuration and the excited states are states with flipped spins. Finite values of κ will lower energies of some of the excited states, but the all 'up' (or all 'down') state is the lowest in energy until $\kappa = \frac{1}{2}$ when all the states having no single spin surrounded by opposite spins have the same energy. For $\kappa > \frac{1}{2}$ '...up-up-down-down...' state crosses all other states to become

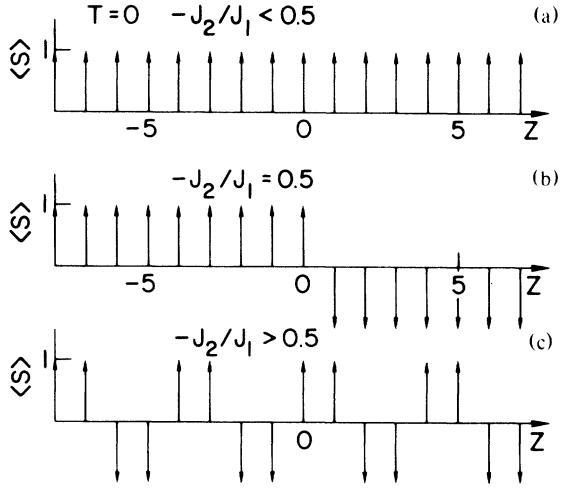

Figure 3.4: The ground state spin configuration of the ANNNI model. (a) $0 < \kappa = -\frac{J_2}{J_1} < \frac{1}{2}$, the ground state is ferromagnetic. (b) At $\kappa = \frac{1}{2}$ there are many ground states possible, one of them shown here. (c) For $\kappa > \frac{1}{2}$, 'up-up-down-down' state (also known as (2,2)-'antiphase' or simply 'antiphase') is the ground state. (from ref [3])

the new ground state and it remains the same for all larger values of κ. Hence the transition is a first order transition and is brought about by a level crossing. ***Degeneracy at the Multiphase Point: Transfer Matrix Method***: The point $\kappa = \frac{1}{2}$ is a multiphase point where any spin configuration with more than one spins of same sign side by side is a ground state. The degeneracy of ground states at this point can be calculated using transfer matrix method. We note that the Boltzmann weight at $T = 0$ is 1 for any ground state and 0 for all excited states. Hence the partition function

$$\begin{aligned} Z &= \sum_{\text{all configurations}} e^{-\frac{E}{k_B T}} \\ &= \nu(0) \end{aligned} \tag{3.3}$$

where $\nu(0)$ is the degeneracy of the ground states ($E = 0$). Now, we work out the partition function using transfer matrix method. At this point it is convenient to map this model onto an Ising model with nearest neighbour antiferromagnetic interaction in an external field using the substitution $\sigma_i = S_i S_{i+1}$. Then the

3.3 Ground State of the Model and Low Temperature Phase Diagram

ANNNI Hamiltonian (3.1) transforms to

$$H = -J_1 \sum_i \sigma_i - J_2 \sum_i \sigma_i \sigma_{i+1}. \tag{3.4}$$

Here we have written the Hamiltonian in the form of a one dimensional spin system and left the in plane contribution to the energy, as we argued earlier.

Now, using standard transfer matrix method the Hamiltonian is given by

$$H = Trace(\mathbb{T}^L), \tag{3.5}$$

L being the system size i.e., number of sites along $z-$axis. The 2×2 transfer matrix $\mathbb{T}$ is given by,

$$\mathbb{T} = \begin{array}{c} \\ \uparrow \\ \downarrow \end{array} \begin{array}{c} \begin{array}{cc} \uparrow & \downarrow \end{array} \\ \begin{pmatrix} 1 & 1 \\ 1 & 0 \end{pmatrix} \end{array}. \tag{3.6}$$

We note that at the multiphase point spin configurations having one spin surrounded by opposite spins are not allowed (e.g. $S_i{=}\uparrow$, $S_{i+1}{=}\downarrow$ $S_{i+2}{=}\uparrow$) and hence in our transformed variable σ the matrix entry corresponding to ($\sigma_i = S_i S_{i+1} {=}\downarrow$, $\sigma_{i+1} = S_{i+1} S_{i+2} {=}\downarrow$) is zero.

The characteristic equation for the eigen values of $\mathbb{T}$ is given by,

$$\begin{aligned} \begin{vmatrix} 1-\lambda & 1 \\ 1 & -\lambda \end{vmatrix} &= 0 \\ \Rightarrow \lambda^2 - \lambda - 1 &= 0. \end{aligned} \tag{3.7}$$

The solutions of (3.7) are non degenerate and the larger one is $\lambda_1 = \frac{1+\sqrt{5}}{2} (= \mu,$ the Golden Ratio), the smaller one is $\lambda_2 = \frac{1-\sqrt{5}}{2}$. Hence, by virtue of (3.5),

$$\begin{aligned} Z &= Trace(\mathbb{T})^L \\ &= {\lambda_1}^L + {\lambda_2}^L \\ &= {\lambda_1}^L \left(1 + (\frac{\lambda_2}{\lambda_1})^L\right) \\ &= \mu^L, \text{as } L \to \infty \\ \Rightarrow \nu(0) &= \mu^L. \end{aligned} \tag{3.8}$$

The last step follows from (3.3).

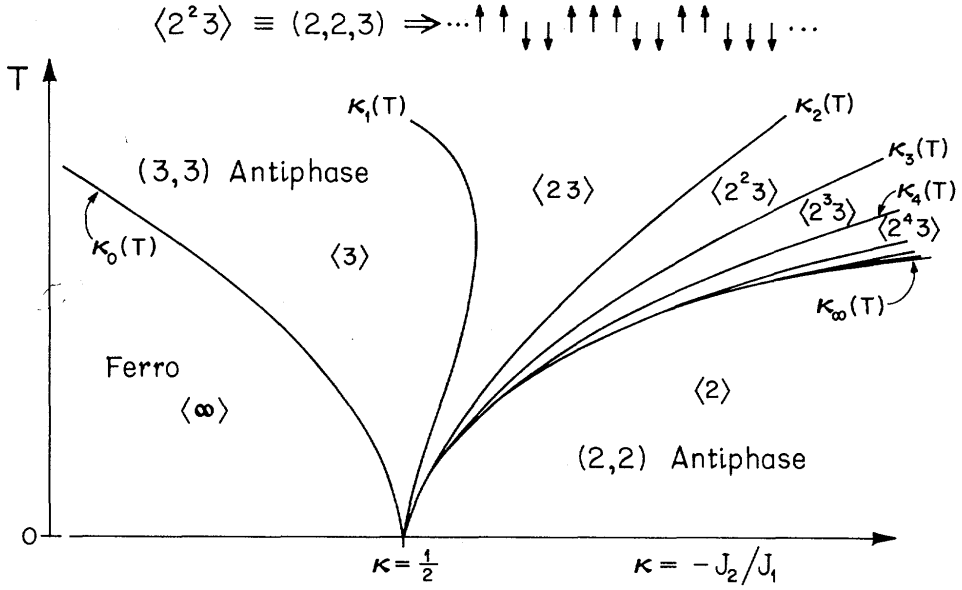

Figure 3.5: Low temperature sequence of phases of the ANNNI model. (taken from ref [4])

Without going to the transformed variable, it is also possible to calculate the partition function. In that case we can take blocks of two spins and transfer it to the next block of two spins. The transfer matrix is 4×4 then and the partition function $Z = Trace(\mathbb{T}^{\frac{L}{2}})$.
The entropy of the system is $\mathcal{S} = L \ln \mu$, but entropy per spin

$$\frac{\mathcal{S}}{LM} = \frac{L \ln \mu}{LM} \to 0$$

as $L, M \to \infty$, M being the number of sites in a plane perpendicular to the $z-$axis.

3.3.2 Low temperature phase diagram: sequence of phases

The low temperature phase diagram of the ANNNI model was studied by Michael Fisher and Walter Selke [5]. They found that from the highly degenerate multiphase point ($\kappa = \frac{1}{2}, T = 0$), lots of phases spring out at finite temperature.

The low temperature phase diagram can be obtained by systematic low temperature expansion in the variables $w = e^{-2K_0}$ and $x = e^{-2K_1}$, the elementary

Boltzmann factors where $K_0 = \frac{J_0}{k_B T}$ and $K_1 = \frac{J_1}{k_B T}$. Near the multiphase point

$$\kappa = \frac{1}{2} + \delta > 0, \tag{3.9}$$

where δ is small and measures the deviation from the multiphase point along κ axis. $\delta = 0$ corresponds to the multiphase point at $T = 0$.

Notation: Before we proceed to the low temperature expansion calculations let us explain the notation. We define structural variables $L_k = Ll_k$ as the number of spin bands of length k,L being the system size along the $z-$axis. A spin band is surrounded by bands of opposite spins. The variables $\{l_k\}$ satisfy the following constraints

$$\sum_{k\geq 0} kl_k = 1 \tag{3.10}$$

and

$$l_k \geq 0 \tag{3.11}$$

For a detailed analysis of the process the original paper [5] is referred. Here we present the main scheme of the treatment.

Expansion of Partition Function about a Ground State: As the temperature is raised from $T = 0$ some of the spins will be flipped from the ground state configuration. The partition function can be expanded about a given ground state structure ($\{l_k\}$) as

$$Z_N\{l_k\} = e^{-\frac{NE_0\{l_k\}}{k_B T}}[1 + \sum_{n=1} \Delta Z_N^{(n)}]. \tag{3.12}$$

E_0 is the energy per spin in the ground state and the second term in the square bracket in (3.12) is the contribution due to various number n of flipped spins.

In the following we list various environments of a spin we need to consider in order to calculate their contribution to the ground state energy. Energy contribution to ground state per spin and number of each type of spins in a given sequence ($\{l_k\}$) are given.

3.3 Ground State of the Model and Low Temperature Phase Diagram

Description of the configuration	Symbol	Energy,ΔE_λ, in excess to the in-layer contribution -$\frac{1}{2}q_\perp J_0$	No. of such spins in a given sequence $\{l_k\}$, N_k
Bulk spin $(\uparrow\uparrow\hat{\uparrow}\uparrow\uparrow)$	o	$-\frac{1}{2}(1-2\delta)J_1$	$N\sum_{k\geq 5}(k-4)l_k$
Near edge spin $(\uparrow\uparrow\hat{\uparrow}\uparrow\downarrow)$	π	$-J_1$	$N\sum_{k\geq 4}2l_k$
Centre spin $(\downarrow\uparrow\hat{\uparrow}\uparrow\downarrow)$	ρ	$-\frac{1}{2}(3+2\delta)J_1$	Nl_3
Edge spin $(\uparrow\uparrow\hat{\uparrow}\downarrow\downarrow)$	σ	0	$N\sum_{k\geq 3}2l_k$
Two band spin $(\downarrow\uparrow\hat{\uparrow}\downarrow\downarrow)$	τ	$-\frac{1}{2}(1+2\delta)J_1$	$2Nl_2$

Combining all these the ground state energy can be written

$$\begin{aligned} E_0\{l_k\} &= -\frac{1}{2}q_\perp J_0 + \Delta E_\lambda N_\lambda \\ &= -\frac{1}{2}q_\perp J_0 - \frac{1}{2}J_1 - J_1\delta[2l_2 + l_3 - \sum_{k\geq 5}(k-4)l_k] \end{aligned} \tag{3.13}$$

subject to the constraints (3.10) and (3.11). In any ground state $l_1 = 0$. This is because an 'up'-spin surrounded by two 'down'-spins can be obtained by flipping the middle one of three consecutive 'down'-spins. Now the next nearest neighbours can be either both 'up', or both 'down' or one 'up' one 'down'. In all the three cases the energy cost is positive for $-\frac{3}{2} < \delta < \frac{1}{2}$.

When the spins as listed in the table are flipped the energy change for each type of spin becomes,

$$\epsilon_\lambda = 2q_\perp J_0 - 4\Delta E_\lambda. \tag{3.14}$$

Hence the relevant Boltzmann factors in terms of the variables w and x are $w^{q_\perp}x^{1-2\delta}, w^{q_\perp}x^2, w^{q_\perp}x^{3+2\delta}, w^{q_\perp}, w^{q_\perp}x^{1+2\delta}$ corresponding to types $o, \pi, \rho, \sigma, \tau$ respectively. Also,

$$\begin{aligned} \frac{\Delta Z_N^{(1)}}{N} &= \sum_\lambda (\frac{N_\lambda}{N})e^{-\frac{\epsilon_\lambda}{k_B T}} \\ &= w^{q_\perp}\Bigg(x^{1-2\delta}\sum_{k\geq 5}(k-4)l_k + 2x^2\sum_{k\geq 4}l_k + x^{3+2\delta}l_3 \\ &\qquad + 2\sum_{k\geq 3}l_k + 2x^{1+2\delta}l_2\Bigg) \end{aligned} \tag{3.15}$$

We can now calculate the variational free energy for $(\{l_k\})$ and then minimize the free energy with respect to $(\{l_k\})$.

The reduced free energy per spin

$$\begin{aligned} f\{l_k\} = \frac{F\{l_k\}}{Nk_BT} &= -\frac{1}{N} ln Z_N\{l_k\} \\ &= \frac{E_0\{l_k\}}{k_BT} - \frac{\Delta Z_N^{(1)}}{N} + \mathcal{O}\left(w^{2q_\perp - 2}\right). \end{aligned} \tag{3.16}$$

Using (3.13) and (3.15),

$$\begin{aligned} f\{l_k\} &= -\frac{1}{2}q_\perp K_0 - \frac{K_1}{2} - \frac{K_1\delta}{3} + \frac{1}{3}w^{q_\perp}\left(x^{3+2\delta} + 2\right) \\ &\quad + a_2^{(1)}(\delta) l_2 + \sum_{k\geq 4} k a_k^{(1)}(\delta) l_k \end{aligned} \tag{3.17}$$

where

$$a_2^{(1)}(\delta) = -\frac{4}{3}K_1\delta + \frac{2}{3}w^{q_\perp}\left(x^{3+2\delta} + 2 - 3x^{1+2\delta}\right) \tag{3.18}$$

$$\begin{aligned} k a_k^{(1)}(\delta) &= \frac{4}{3}K_1\delta(k-3) - w^{q_\perp}\left((k-4)x^{1-2\delta} + 2x^2 - \right. \\ &\quad \left. \frac{k}{3}x^{3+2\delta} - \frac{2}{3}(k-3)\right). \end{aligned} \tag{3.19}$$

The last expression is for $k \geq 4$.

Minimization of the Free Energy: We note that $a_2^{(1)}(\delta)$ is negative for $\delta > \delta_1^{(1)}$ where $\delta_1^{(1)}$ is defined through the equation

$$a_2^{(1)}(\delta_1^{(1)}(T)) = 0. \tag{3.20}$$

On the other hand $a_k^{(1)}(\delta)$ is negative for $\delta < \delta_{-\infty}^{(1)}$ where $\delta_1^{(1)}$ is defined through the equation

$$a_k^{(1)}(\delta_\infty^{(1)}(T)) = 0. \tag{3.21}$$

Now, for $\delta > \delta_1^{(1)}$,$a_2^{(1)}(\delta) < 0$ and hence the minimum of free energy (3.17) is obtained by having maximum number of 2-bands, i.e., $l_2 = \frac{1}{2}$ and this indicates that for $\delta > \delta_1^{(1)}$ the 'antiphase' is stable. for $\delta < \delta_{-\infty}^{(1)}$, the minimum of free energy is obtained by putting $Ll_\infty = 1$ and all other $l_k = 0$, showing a ferromagnetic phase.

In between these limits, for $\delta_{-\infty}^{(1)} < \delta < \delta_1^{(1)}$ both $a_2^{(1)}(\delta)$ and $a_k^{(1)}(\delta), k \geq 4$ are positive and hence the minimum free energy is obtained by putting $l_2 = 0, l_k = 0$

for $k \geq 4$,$l_3 = \frac{1}{3}$ so that a new phase (... $\uparrow\uparrow\uparrow\downarrow\downarrow\downarrow$ ...) interpolates between the $< \infty >$ and $< 2 >$ phase.

Ferromagnetic to $< 3 >$ ***Transition***: By equating the free energies of $< \infty >$ and $< 3 >$ phases the phase boundary is obtained. The calculation of the phase boundary can be improved by considering higher orders of w corresponding to multiple spin flip.

The order of transition from $< \infty >$ to $< 3 >$ can be found out by looking at the surface energy $\Sigma_0(x, w, \delta)$ when a surface is created by inserting some three-'up'-three-'down' spin patches in an all-'up' environment. Upto $\mathcal{O}(w^{q_\perp})$ the surface tension is

$$\frac{\Sigma_0}{k_B T} \approx \frac{1}{2} w^{q_\perp} x(1-x)^2 \tag{3.22}$$

so that for the entire range of $x, 0 < x < 1$ the surface tension is positive, thereby showing that the transition is of first order.

It is to be noted that the complete phase diagram as calculated by Monte Carlo and other methods show that the ferromagnetic phase can coexist with $< 3 >$ phase upto a temperature $T = T_F$ above which there are transitions from ferromagnetic to other sinusoidally ordered phases. However, the transition remains first order all the way upto the Lifshitz point.

Low Temperature Sequence of Phases: It is important to note that at the other phase boundary, namely that between $< 3 >$ and $< 2 >$, $a_2^{(1)}(\delta) = 0$ and hence all the states consisting of length two and three bands coexist on this line. This degeneracy is lifted when we consider contribution from multiple spin flips. A calculation similar to the previous one at the next higher order in w reveals that a new phase $< 23 >$ becomes stable for some range of $\delta(T)$ in between $< 3 >$ and $< 2 >$ states. Again we find that there is a degeneracy at the boundary of this new phase and $< 2 >$, the antiphase. At the next order, another phase, namely $< 2^2 3 >$ is found to interpolate between $< 23 >$ and $< 2 >$ phase.

Thus we find the sequence of phases as $< \infty >, < 3 >, < 23 >, < 2^2 3 >, < 2^3 3 >, ..., < 2^{j-1} 3 >, ..., < 2 >$, j being a positive integer when we move from the ferromagnetic phase to the right at a fixed low temperature in the phase diagram. Conversely if we start from the 'antiphase' state at $T = 0$ and close to the multiphase point and then move to higher temperatures keeping δ fixed, we

encounter the phases in reverse i.e.,$< 2 >, ..., < 2^{j-1}3 >, ..., < 2^2 3 >, < 23 >, < 3 >$. This is easy to check from fig (3.5).

Comments: A few comments are in order:

(i) The width of the phases (of $< 2^{j-1}3 >$ type) decreases with increasing j. The boundary lines are given by,

$$\kappa_{j+1}(T) - \kappa_j(T) \sim w^{q_\perp j}. \tag{3.23}$$

(ii) The wave vector characterising the states are given by,

$$2\pi q_j = \frac{\pi j}{(2j+1)}, \ j = 1, 2, 3, ... \tag{3.24}$$

As $j \to \infty$, the wave vector varies as,

$$q_\infty - q(T, \kappa) \sim \frac{1}{\ln\{[\kappa_\infty(\mathrm{T}) - \kappa]^{-1}\}}. \tag{3.25}$$

(iii) At relatively higher temperatures states of $< 2^{j-1}32^j 3 >$ and other complicated form exists. If we treat the 3-bands as walls placed within 2-band spins, various interactions between the walls namely 2-wall, 3-wall, ..., n-wall interactions need to be considered carefully in order to find out for other possible stable phases [[19],[20],[21]].

3.4 High Temperature Phase Diagram

For finite values of κ, at high enough temperatures a paramagnetic phase is expected. As the temperature is lowered we might come across an instability in the paramagnetic phase against a ferromagnetic or a spatially modulated phase with wave vector $\vec{q}$. The instability is expected to show up as a divergence in the susceptibility $\chi(\vec{q}, T)$. The susceptibility $\chi(\vec{q}, T)$ is defined in the following way. We put an external field h_0 at one site only in the uniformly ordered phase. Then the translational invariance of the phase is broken. However, if the field is small enough, we can break up the magnetization at i^{th} site as a sum of an average

magnetization plus a small fluctuation about that average, i.e., $m_i = m + \delta m_i$. $\chi(\vec{q}, T)$ is defined as,

$$\chi(\vec{q}, T) = \lim_{h_0 \to 0} \frac{\delta m_{\vec{q}}}{h_0} \tag{3.26}$$

where $\delta m_{\vec{q}}$ is the Fourier transform of δm_i at wave vector $\vec{q}$. Hence this susceptibility measures the response due to a localised infinitesimal field.

3.4.1 Instability of the paramagnetic phase

Within the Ornstein-Zernike theory the mean field susceptibility $\chi(\vec{q}, T)$ in the disordered phase is given by the following expression:

$$\chi(\vec{q}, T) = \frac{\beta}{1 - \beta \mathcal{J}(\vec{q})} \tag{3.27}$$

where $\beta = \frac{1}{k_B T}$,k_B is the Boltzmann constant. Taking the wave vector $\vec{q}$ of the form $2\pi(0, 0, q)$,

$$\mathcal{J}(\vec{q}) = 4J_0 + 2J_1 \cos 2\pi q + 2J_2 \cos 4\pi q \tag{3.28}$$

So, the paramagnetic susceptibility diverges first when $1 - \beta_c \mathcal{J}(\vec{q_c}) = 0$, where $\vec{q} = \vec{q_c}$ maximizes $\mathcal{J}(\vec{q})$.

i.e.,

$$k_B T_c = 4J_0 + 2J_1 \cos 2\pi q_c + 2J_2 \cos 4\pi q_c \tag{3.29}$$

Here q_c is obtained by maximizing (3.28) with respect to q.

$$2\pi q_c = \arccos \frac{1}{4\kappa} \tag{3.30}$$

Equation (3.30) restricts the values of κ in order to obtain a real q_c. Since $\cos q_c < 1$, $\kappa > \frac{1}{4}$. For $\kappa < \frac{1}{4}$, $q_c = 0$ maximizes (3.28). This shows a transition from the paramagnetic to a ferromagnetic phase for $\kappa < \frac{1}{4}$.

Inserting (3.30) into (3.29) we get the mean field phase boundary for paramagnetic to modulated phase transition,

$$k_B T_c = 4J_0 + J_1 \left(2\kappa + \frac{1}{4\kappa}\right), \ \kappa > \frac{1}{4}. \tag{3.31}$$

whereas, the mean field boundary between paramagnetic phase and ferromagnetic phase is obtained by putting $q_c = 0$ in (3.29) and it is,

$$k_B T_c = 4J_0 + J_1 (2 - 2\kappa), \ \kappa \leq \frac{1}{4}. \tag{3.32}$$

The mean field transition lines are shown approximately in fig (3.6).

3.4.2 Instability of the ferromagnetic phase

Within the ferromagnetic phase we can use Ornstein-Zernike expression for mean field susceptibility:

$$\chi(\vec{q}, T) = \frac{(1 - m^2)\beta}{1 - (1 - m^2)\beta \mathcal{J}(\vec{q})} \tag{3.33}$$

where m is the magnetization per site at temperature T. An estimate of m could be obtained by minimizing Landau free energy functional per spin F. Within the ferromagnetic phase,

$$F(m, T) = -\frac{1}{2} (\mathcal{J}(0) - k_B T) m^2 + \frac{k_B T}{12} m^4 \tag{3.34}$$

upto fourth order in m. Minimizing $F(m, T)$ w.r.t m, we get the squared spontaneous magnetization

$$m^2 = \frac{3 (\mathcal{J}(0) - k_B T)}{k_B T} \tag{3.35}$$

Now that we have an estimate of m, we can look at the wave vector $q = q_c$ for which the susceptibility in (3.33) first diverges. When it happens, the ferromagnetic phase will be unstable against the modulated phase corresponding to that wave vector.The criterion for the instability is,

$$1 - (1 - m^2)\beta_c \mathcal{J}(\vec{q_c}) = 0. \tag{3.36}$$

Hence using (3.35) in (3.36) we get the phase boundary by solving the following equation for T_c as a function of κ,

$$(4 - 3\beta_c \mathcal{J}(0)) \beta_c \left(4J_0 + J_1 \left(\frac{1}{4\kappa} + 2\kappa \right) \right) = 1 \tag{3.37}$$

This expression for the transition line is based on an estimate of m which was assumed to be small, so that we neglected higher orders in m in (3.34). Hence

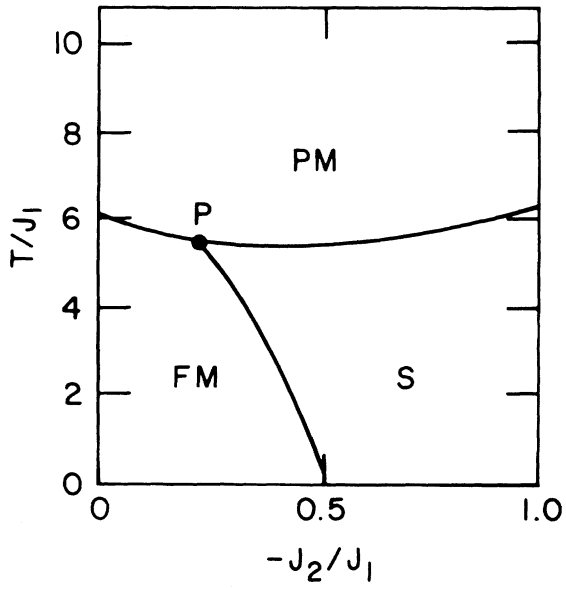

Figure 3.6: The transition lines in the phase diagram of the ANNNI model shown approximately with $J_0 = J_1$. (from ref [3])

we can trust this result close to the Lifshitz point. It is to be noted that on this transition line, magnetization does not go to zero and this shows that the phase transition from the ferromagnetic to the spatially modulated phase is first order in nature, at least close to Lifshitz point[1]. At the Lifshitz point ferromagnetic phase, paramagnetic phase and spatially modulated phase coexist and hence the jump in the magnetization vanishes. The wave vector for which the instability occurs is given by (3.30) as a function of κ.

3.4.3 Mean field theory and the soliton picture

The phase diagram at high temperatures can be analyzed using a mean field theory. One starts by assuming a mean field Hamiltonian

$$\mathcal{H}_{MF} = -\sum_i H_i S_i + \frac{1}{2} H_i < S_i >, \tag{3.38}$$

[1]In section (3.3.2) it was pointed out that the whole phase boundary between ferromagnetic to modulated phase, from the multiphase point to the Lifshitz point is of first order in nature.

$< S_i >$ being the thermal average of the spin at i^{th} layer,$i = 1, 2, ..., L$. $\mathrm{H_i}$ is the effective field at i arising from the interactions with surrounding spins. Minimization of trial free energy leads to the self consistent sets of equation,

$$< S_i >= \tanh(\beta \mathrm{H_i}) \tag{3.39}$$

$$H_i = \sum_j J_{ij} < S_j > . \tag{3.40}$$

Unlike in the case of Ising model with nearest neighbour ferromagnetic coupling, these sets of equations cannot be reduced to just a couple of equations for we cannot use translational invariance in general for spatially modulated phases. It turns out to be very difficult task to solve these self-consistent equations. However,they can be analyzed in the following way.

If we suppose that the spin sequence repeats after L sites along $z-$axis, the free energy per site becomes,

$$F(L,T) = -\frac{1}{L\beta} \sum_{j=o}^{L-1} \ln \mathrm{Tr}\ \mathrm{e}^{-\beta \mathcal{H}_{\mathrm{MF}}}. \tag{3.41}$$

This free energy is minimized w.r.t. L numerically. In principle the calculation should be performed upto $L \to \infty$ in order to allow for any possible incommensurate phase. But in practice numerical calculation upto L=17 were carried out [3]. Most of the phase diagram is filled up by various commensurate phases. Near the paramagnetic transition line this numerical mean field theory fails.

Important Features of the Modulated Phases as Found by Mean Field Theory: Fig (3.7) shows wave vector vs temperature for $\kappa = 0.6$ and $\kappa = 0.7$. The following points are interesting to note:

(i) Most of the phase diagram is filled by the wave vectors $q = \frac{1}{4}$, $\frac{1}{5}$ and $\frac{1}{6}$.

(ii) Some wave vectors are stable only for a very small temperature range.e.g. $q = \frac{2}{9}$ is stable for a temperature range $\Delta T \simeq 0.0004 T_c$.

(iii) Some of the wave vectors do not occur at all as stable phase, like q jumps from $\frac{2}{11}$ to $\frac{1}{6}$ without assuming the value $\frac{3}{17}(= \frac{2+1}{11+6})$. Hence the 'Devil's staircase' is not complete.

(iv) For $\kappa = 0.6$ the wave vector vs temperature curve is not monotonic.

Most of the features of the wave vector vs T curve can be understood within a soliton picture. The basic scheme of the soliton picture is portrayed here.

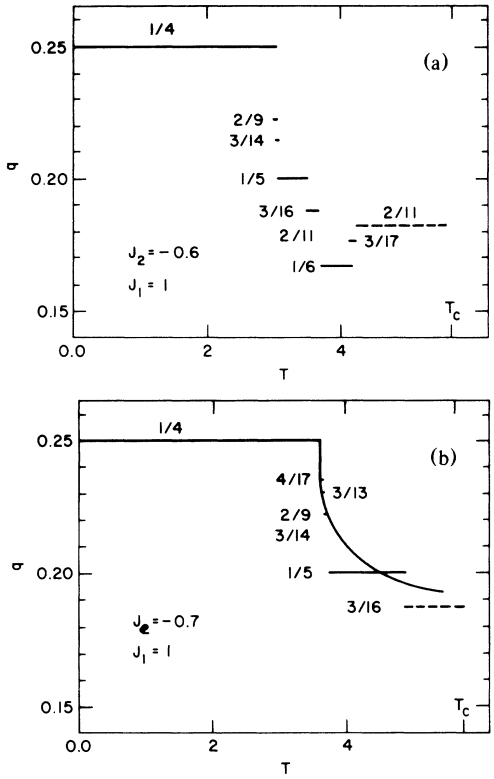

Figure 3.7: Wave vector vs temperature for (a)$\kappa = 0.6$ and (b)$\kappa = 0.7$ as calculated numerically by Bak and Boehm [3]

If F be the Landau functional in the presence of an external field H_{ext},then

$$\frac{\delta F}{\delta < S_i >} = H_{ext}(< S_i >). \tag{3.42}$$

Hence,

$$\begin{aligned} < S_i > &= \tanh \beta \left(\mathrm{H_i} + \mathrm{H_{ext}}\right) \\ &= \tanh \beta \left(\sum_{\mathrm{j}} \mathrm{J_{ij}} < \mathrm{S_j} > + \mathrm{H_{ext}}\right) \end{aligned} \tag{3.43}$$

so,

$$H_{ext} = -\sum_j J_{ij} < S_j > + \frac{1}{\beta} \tanh^{-1} < S_i > . \tag{3.44}$$

Hence, using (3.42), we get,

$$F = -\frac{1}{2L}\sum_{j} J_{ij} < S_i >< S_j > + \frac{1}{L\beta}\sum_{i} \int_{0}^{<S_i>} \tanh^{-1}\,\sigma\; \mathrm{d}\sigma. \tag{3.45}$$

Expanding the free energy in powers of $S_{\vec{q}}$, the Fourier transform of $< S_i >$, we get

$$F = -\frac{1}{2}\sum_{\vec{q}}[\mathcal{J}(\vec{q})-T]S_{\vec{q}}S_{-\vec{q}} + \frac{T}{12}\sum_{\tau}\sum_{\vec{q1}}\cdots\sum_{\vec{q4}} S_{\vec{q1}}S_{\vec{q2}}S_{\vec{q3}}S_{\vec{q4}}\,\delta(\vec{q_1}+\vec{q_2}+\vec{q_3}+\vec{q_4}-\vec{\tau}) + \mathcal{O}(S^6_{\vec{q}}). \tag{3.46}$$

Here τ is a reciprocal lattice vector and its presence reflects the basic fact that the spins are sitting on a lattice.

Free Energy near the $q = \frac{1}{4}$ ***Phase***: To find the stability of the phase with wave vector $q_0 = \frac{1}{4}$ we expand the free energy about $q = q_0 = \frac{1}{4}$.

Let us define $S_{\frac{1}{4}}(\vec{r})$ and $S_{-\frac{1}{4}}(\vec{r})$ as,

$$S_{\frac{1}{4}}(\vec{r}) = \sqrt{2}\left(\frac{1}{2\pi}\right)^3 \int d\vec{q}\; e^{i\vec{q}.\vec{r}} S_{-\vec{q_0}+\vec{q}} \tag{3.47}$$

$$S_{-\frac{1}{4}}(\vec{r}) = \sqrt{2}\left(\frac{1}{2\pi}\right)^3 \int d\vec{q}\; e^{-i\vec{q}.\vec{r}} S_{-\vec{q_0}-\vec{q}}. \tag{3.48}$$

$S_{\frac{1}{4}}(\vec{r})$ describes a spin density wave

$$S(\vec{r}) = \frac{1}{\sqrt{2}} S_{\frac{1}{4}}(\vec{r}) e^{2\pi i(\frac{z}{4})}. \tag{3.49}$$

The last term arises from Umklapp terms. Also, because the wave vector $\vec{q}$ has only z-component, $S_{\frac{1}{4}}(\vec{r})$ depends on z only.

If we assume that near the commensurate phase ($q = \frac{1}{4}$) the amplitude of the order parameter $S_{\pm\frac{1}{4}}(z)$ while the phase ($\phi(z)$) is allowed to vary with z [[12],[22],[23]],

$$S_{\pm\frac{1}{4}}(z) = A\; e^{i\phi(z)}. \tag{3.50}$$

The commensurate phase is given by (3.49) and (3.50) with ϕ = constant. The amplitude A might be obtained by minimizing the Landau functional in the commensurate phase.

If we choose $\phi(z) = \eta z$, this describes an incommensurate modulated phase. The free energy takes the form [3],

$$F = \int dz\ cA^2 \left[\frac{1}{2} \left(\frac{d\phi}{dz} - \eta \right)^2 + \nu(1 + cos\ p\phi) \right] \tag{3.51}$$

with $p = 4, \eta = -\frac{1}{4\kappa}, \nu = -\frac{k_B T A^2}{96 J_2}$.

This is of the same form as the energy of FVdM model discussed in Chapter 2.

The first term in (3.51) favours $\phi = \eta z$, i.e., an incommensurate phase while the second term favours $\phi = \frac{\pi}{4}$, the commensurate phase.

Sine-Gordon Equation as the Minimization Condition for Free Energy: The solitonic solutions: Minimizing the free energy leads to the Sine-Gordon equation,

$$\frac{d^2\phi}{dz^2} + 4\nu\ sin\ 4\phi = 0. \tag{3.52}$$

One of the solution of (3.52) is given by,

$$\phi(z) = \frac{\pi}{4} - \tan^{-1}\ \mathrm{e}^{4\sqrt{\nu}z} \tag{3.53}$$

and this represents an anti-soliton. In general the solution is given by a set of regularly spaced soliton or a 'soliton lattice' with lattice constant l such that,

$$\bar{q} = \frac{2\pi}{pl}, \tag{3.54}$$

$\bar{q}$ being the deviation of the average wave vector from q_0 in z-direction.

The solitons can be thought of as walls between commensurate phases. Near the commensurate phase, the free energy takes the asymptotic form,

$$\frac{F}{cA^2} = \left(4\frac{\sqrt{\nu}}{\pi} - |\eta| \right) \bar{q} + \frac{16\sqrt{\nu}}{\pi} \bar{q}\ exp\left(-\frac{2\pi\sqrt{\nu}}{\bar{q}} \right). \tag{3.55}$$

The first term can be thought of as soliton formation energy and the second term as a weak repulsion between the solitons.

A phase with $q = \frac{1}{5}$ may be regarded as a phase with one soliton inserted every period,that with $q = \frac{3}{13}$ as a phase with one soliton every three periods etc.

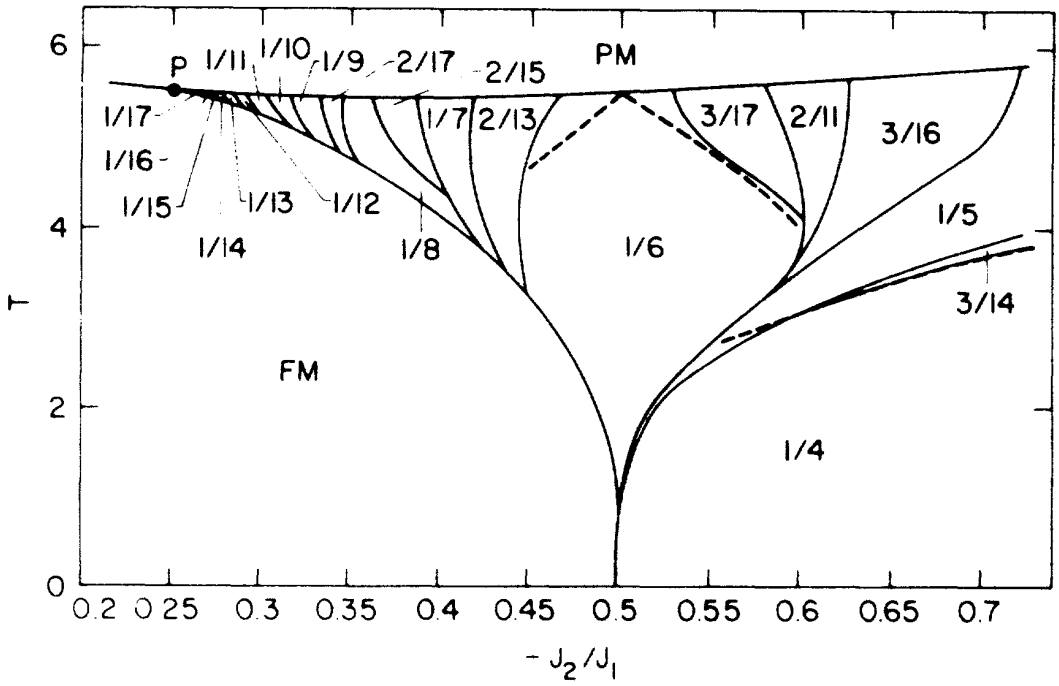

Figure 3.8: The phase diagram of ANNNI model in 3 dimensions as found out by Bak and Boehm using mean field numerical calculations (ref [3])

For small ν or large $|\eta|$, the soliton formation energy goes negative and hence the commensurate phase becomes unstable against formation of an incommensurate phase.

The transition temperature is obtained from (3.55) as a function of J_1 and J_2,

$$k_B T_{CI} = 4J_1 - 2J_2 + \frac{\pi^2 J_1^2}{8J_2} \tag{3.56}$$

The soliton formation energy remains positive for a large range of T and κ, showing the stability of the phase.

In a similar treatment the Landau free energy can be written about other stable wave vectors like $q = \frac{1}{6}$. The phase boundary as calculated using the soliton picture matches well with other numerical studies. The phase diagram as found out numerically is shown in fig (3.8).

Crucial Features of the Phase Diagram in One and Two Lattice Dimensions: The phase diagram in one lattice dimensions can be solved exactly using transfer matrix method. At T=0, entropy per spin does not vanish in 1-D. In the thermodynamic limit, the entropy per site becomes,

$$\begin{aligned} \frac{\mathcal{S}}{L} &= \frac{L \ln \mu}{L} \\ &= \ln \mu \end{aligned} \tag{3.57}$$

as $L \to \infty$. This differs from the case in higher dimensions.

Also long range order is destroyed in 1-D for finite temperature as can be seen from the exponential decay in the spin spin correlation function. In the phase diagram there exists local spatially modulated phases but the stability of these phases get enhanced in higher dimensions because of the in-layer spins coupled ferromagnetically.

In 2-D the entropy per spin again vanishes, like in 3-D at T=0 and $\alpha = \frac{1}{2}$. The most interesting feature of the 2-D phase diagram is that the paramagnetic phase touches T=0 axis so that there is always a paramagnetic phase between ferromagnetic and spatially modulated phase. A detailed account is provided at the review article by W. Selke [24].

Summary: To summarise, the phase diagram of ANNNI model is sufficiently rich. It shows a uniformly ordered state, a disordered state and a number of spatially modulated phases (commensurate and incommensurate) that arise out of competition between nearest and next nearest neighbour couplings. Though it involves short range interaction, it does show very long periodic structures.

The infinite sequence of phases shown by ANNNI model provides a motivation to use this model to explain 'polytypism' in closed packed materials, as we shall discuss in the next chapter.

Chapter 4

Polytypes and Application of ANNNI Model to Polytypes

Materials like SiC, ZnS etc having closed packed structures show a wide range of lattice periodicity along some crystallographic axis. This phenomenon is known as 'Polytypism' and results from competing interactions present within the materials. As the temperature, pressure and other chemical environments are changed one polytypic form of these materials can transform to other polytypic forms [[25],[26]].

There are excellent reviews available on Polytypism (for example see Verma and Krishna (1966) [6]). Hundreds of papers in various journals, especially those devoted to crystallography reported new polytypic structures in different materials. Instead of presenting all those information, our aim will be to describe the phenomenon of polytypism briefly, also to look at some plausible explanations of polytypism. We shall try to understand the dynamics of transition from one polytypic structure to another. Since there does not seem to be one general framework for understanding every transformation between polytypic variants, we shall be very specific. We shall pick up a particular transition, namely from 3C to 6H phase and look at the dynamics using Monte Carlo algorithm. First of all let us define polytypism and describe the notations used to represent various polytypes.

4.1 Definition of Polytypism and Notations used

First discovered by Baumhauer [[27],[28]] in SiC, polytypism refers to the ability of a substance to crystallize into a number of different modifications in all of which two dimensions of the unit cell are the same while the third is a variable integral multiple of a common unit [6].

There are various notations available to describe polytypism. The most popular ones are described below:

(a) ***ABC notation***

Various Polytypic modifications can be represented by specifying stacking sequence (A,B,C) of successive closed packed layers. The unit layer of structure might be polyatomic and then the symbols A,B,C represent one kind of atoms, the relative positions of the other being fixed.

(b) ***The Ramsdell notation*** [29]

In this convention the symbols nH or nR means that there are n layers along the c-axis in a unit cell and the symmetry of the crystal is **H**exagonal or **R**hombohedral. 3C is the only structure with cubic symmetry.

(c) ***Zhdanov Symbol***: [30]

The stacking sequence in polytypes can be mapped to a binary variable, 'plus' and 'minus' or 'up' spin and 'down' spin. 'Plus' is assigned at each bond between two neighbouring layers if the letters occur cyclically in ABC notation and 'minus' is assigned when if neighbouring letters is anti-cyclic.

Zhdanov symbol consists of pairs of numbers, the first denoting the number of plus signs and the second denoting the number of minus signs following the plus one. For example 6H is denoted as (3 3). 15R is represented as $(2\ 3)_3$, the subscript 3 denoting that the sequence (2 3) has to be repeated 3-times to complete the unit cell.

4.2 Examples of Polytypism

In more than 40 polytypic structures of SiC, the hexagonal unit cell has $a = b = 3.078$Å, while c is a variable multiple of 2.518Å. The variation of c might be surprising to note. In 2H polytype $c \approx 5$Å.[31] while $c \approx 1500$Å in 594R.[32]

Apart from the hexagonal and rhombohedral modification, known as α-SiC, there is a cubic modification, known as β-SiC [[33],[34]]. Apart from SiC, polytypism is observed in lots of materials. Here are a few notable examples:
(a) ZnS: There are about 200 identified polytypes of ZnS.[35]
(b) CdTe: 2H, 3R, 5H, 6H, 6R, 15R, 3C etc phases are observed.[36]
(c) SnS_2: 2H, 4H, 6H, 18R, 8H, 10H, 22H, 24H, 24R, 30H (or 90R), 36R (or12H), 40H, 72R etc modifications are observed.[37]
(d) CdI_2: About 250 polytypes of this substance has been reported and complete crystal structures of 90 polytypes have been worked out.[38]

Since various polytypes of a material differ only in the stacking sequence along one axis, the bulk densities are almost the same.

4.3 Theories to explain Polytypism

Many theories have been put forward to explain polytypism. An earlier school of thought suggested that polytypism is essentially a non-equilibrium process and arises due to different growth mechanisms (e.g., spiral growth mechanism by Frank 1951 [39]). However, these mechanisms cannot explain the relative stability of various polytypic structures. Jepps and Page [40] characterized several reversible phase transitions between SiC polytypes. This suggested that polytypism might be an equilibrium phenomenon and led people to use equilibrium models to explain it (Price 1983, [41]). The remarkable similarity of SiC polytypes to the infinite sequence of phases found in ANNNI model was a motivation to take this idea seriously [8].

The most abundant phases in common polytypes (like SiC) are obtained in the zero temperature phase diagram of the extended ANNNI model (it involves interactions upto third nearest neighbours). The phase diagram of the extended ANNNI model is shown in fig (4.1). 3C, 4H, 2H and 6H are stable phases at $T = 0$. The 3C-6H transition line is highly degenerate. Here all spin configurations having three or more number of successive spins of same sign are ground states. Hence the degeneracy is exponential in the system size along the stacking axis.

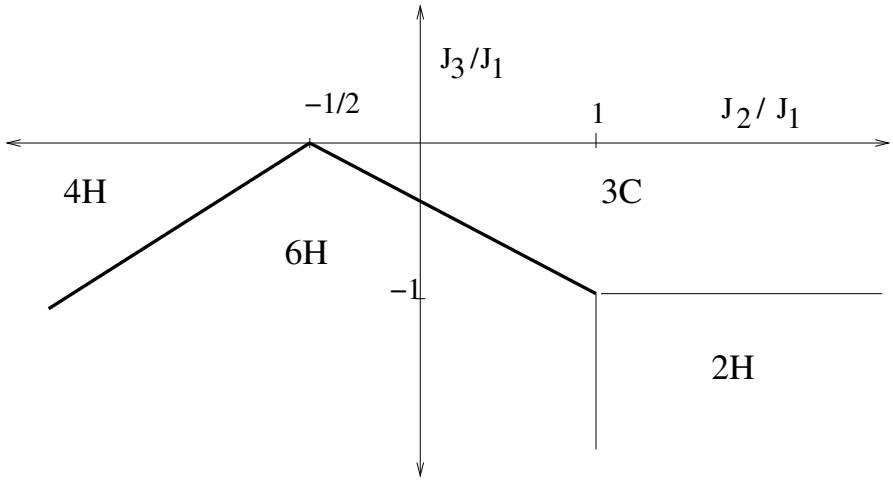

Figure 4.1: Ground state phase diagram of extended ANNNI model. J_i, $i = 1, 2, 3$ are the first, second and third nearest neighbour couplings. $J_1 > 0$ and we have shown only the lower half of the phase diagram since we are interested in 3C-6H phase diagram. On the thick boundaries there are exponentially large degeneracies of ground states.

In the next section we shall use Monte Carlo algorithm[1] at $T = 0$ to look at the transition from 3C to 6H. A similar approach has been adopted by Dhananjai Pandey to study 2H to 6H transformation [42].

4.4 Dynamics of Transformation

In order to study the dynamics of transformation from 3C to 6H phase using Monte Carlo simulation, we have to find out the rules for allowed 'moves' in spin language.

3C: ... A B C A **B C** A B C A **B C** ...
6H: ... A B C A **C B** A B C A **C B** ...

We note that a pair of neighbouring 'B' and 'C' interchanged in this transformation. Now exchange of positions of two atomic layers by coherent movement of all

[1]The Monte Carlo work was done in collaboration with Tridib Sadhu, Department of Theoretical Physics.

the individual atoms seems unlikely to happen in a real system. A more plausible mechanism for the exchange might be that 'cracks' are created in successive B and C layers. By a 'crack' we mean an interface between atoms of B and C positions in a layer. It is important to note that closed packing constraint demands the creation of identical 'cracks' in the neighbouring layers, for otherwise two B's or two C's would be next to each other in the stacking sequence. There is some room for the atoms to move near a 'crack'. This permits ease of motion and leads to the diffusion of the 'crack' by flipping B and C atoms. Thus the layers B and C interchange positions. This seems plausible since the only energy cost is for the creation of the 'crack'; once created it can diffuse almost freely.

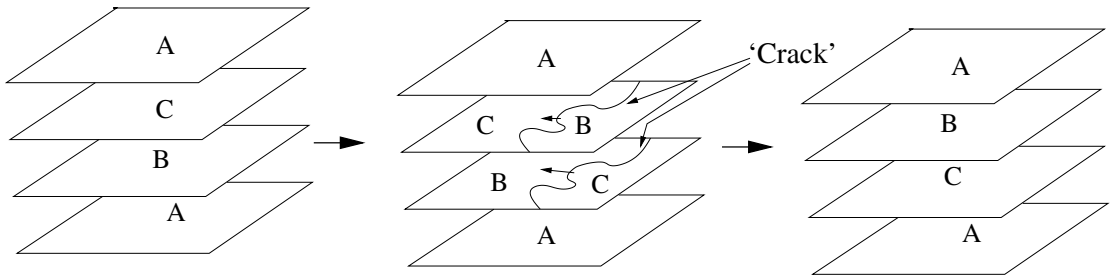

Figure 4.2: A plausible mechanism for interchange of B and C layers. 'Cracks' are formed as a result of B atoms moving to C positions in a plane and C atoms moving to B positions in the neighbouring plane. The crack diffuses to interchange B and C planes.

Dynamics in spin language: In spin language, each move (ABCA→ACBA) consists of a trimer flip.

$$\begin{aligned} \text{3C:} \quad & \ldots \uparrow \uparrow \uparrow \Uparrow \Uparrow \Uparrow \uparrow \uparrow \uparrow \ \ldots \\ \text{6H:} \quad & \ldots \uparrow \uparrow \uparrow \Downarrow \Downarrow \Downarrow \uparrow \uparrow \uparrow \ \ldots \end{aligned}$$

Here for ease of visualization, we have used $\Uparrow$ and $\Downarrow$ instead of $\uparrow$ and $\downarrow$ respectively for the flipped spins. Hence the dynamics we need to consider is the trimer flip dynamics.

We proceed by writing a Monte Carlo code. We consider the system to be at zero temperature. The rules are the following:

(a) start with an initial configuration of one dimensional array of spins,
(b) randomly choose three consecutive spin of same sign (that is all 'up' or all 'down'),
(c) evaluate the energy cost, ΔE of flipping the spins (Extended ANNNI Hamiltonian is used for this).

If $\Delta E < 0$,	the spins are flipped with probability 1.
If $\Delta E = 0$,	the spins are flipped with probability $\frac{1}{2}$.
If $\Delta E > 0$,	the spins are not flipped.

4.5 Results of Monte Carlo: Metastable States

The final state reached under the dynamics was found to be sensitive to the initial configuration. When it was quenched from 3C phase to 6H phase ($J_1 = 0.9, J_2 = 0, J_3 = -0.6$) at $T = 0$, it did not go to the thermodynamically stable 6H phase. Rather, the system went to a locked metastable state. Locally the spin configuration showed 'three-up-three-down' structure but globally the phase was not 6H. For a random initial configuration[1] also the system did not go the thermodynamically stable phase but 'active' and 'frozen' patches of spins were observed for large number of Monte Carlo steps. The 'residual activity' (the number of active spins after large number of Monte Carlo steps) was found not to go to zero even after 800 Monte Carlo steps per site while in the first case it approached zero after ∼200 Monte Carlo steps per site. The result of the Monte Carlo simulation is shown in fig (4.3), at the end of this chapter. Number of sites that remain active after large number of Monte Carlo time steps was found to be proportional to the system size.

When the system was quenched to the multiphase line i.e., the phase boundary between 3C and 6H phases ($J_1 = 0.9, J_2 = 0, J_3 = -0.6$), the spins remained active if started from 3C phase (800 Monte Carlo steps were observed) but went

[1]There is no analogue known to us that corresponds to random configuration in polytypes. However, we might ask a theoretical question whether the dynamics under consideration has dependence on initial configuration. This is the motivation for considering random initial configuration.

to a state with alternate 'frozen' and 'active' spins if started from random configuration (fig (4.5)).

We can rationalize the results for quenching to the degeneracy line in the following way . Since the energy cost of flipping a trimer is zero when it is surrounded by patches of spin of same sign of length greater than two, there might be sites where no move is allowed, e.g., the middle three of an 'up-down-up-down...' configuration of length 9. Next, even if some initial moves are allowed, after some time the system can go a similar configuration to get locked. On the other hand when the system starts from all 'up' configuration, we get only spin patches of length at least three in successive Monte Carlo steps. Hence even if some sites remain inactive for sometime, there is a possibility that it might become active again when the neighbours have flipped to produce energetically favourable conditions.

Discussion: Hence we see that the system might go to a metastable state for some initial configurations. The thermodynamically stable phase is of course lower in energy than any of the metastable states, but in order to reach there, the system has to overcome an activation barrier since the metastable states are at the *local* minima of energy. The time taken to overcome this activation barrier is exponential in the barrier height. The thermodynamically stable state is at the *global* minimum of energy, but reaching it is not easy. The dependence of the final state on the initial configuration is observed for many frustrated systems.

We again emphasize that the actual problem is very complicated. The use of this spin model was motivated from a phenomenological point of view and it did show some interesting properties, which may relate to some aspects of the transformation of polytypic structures.

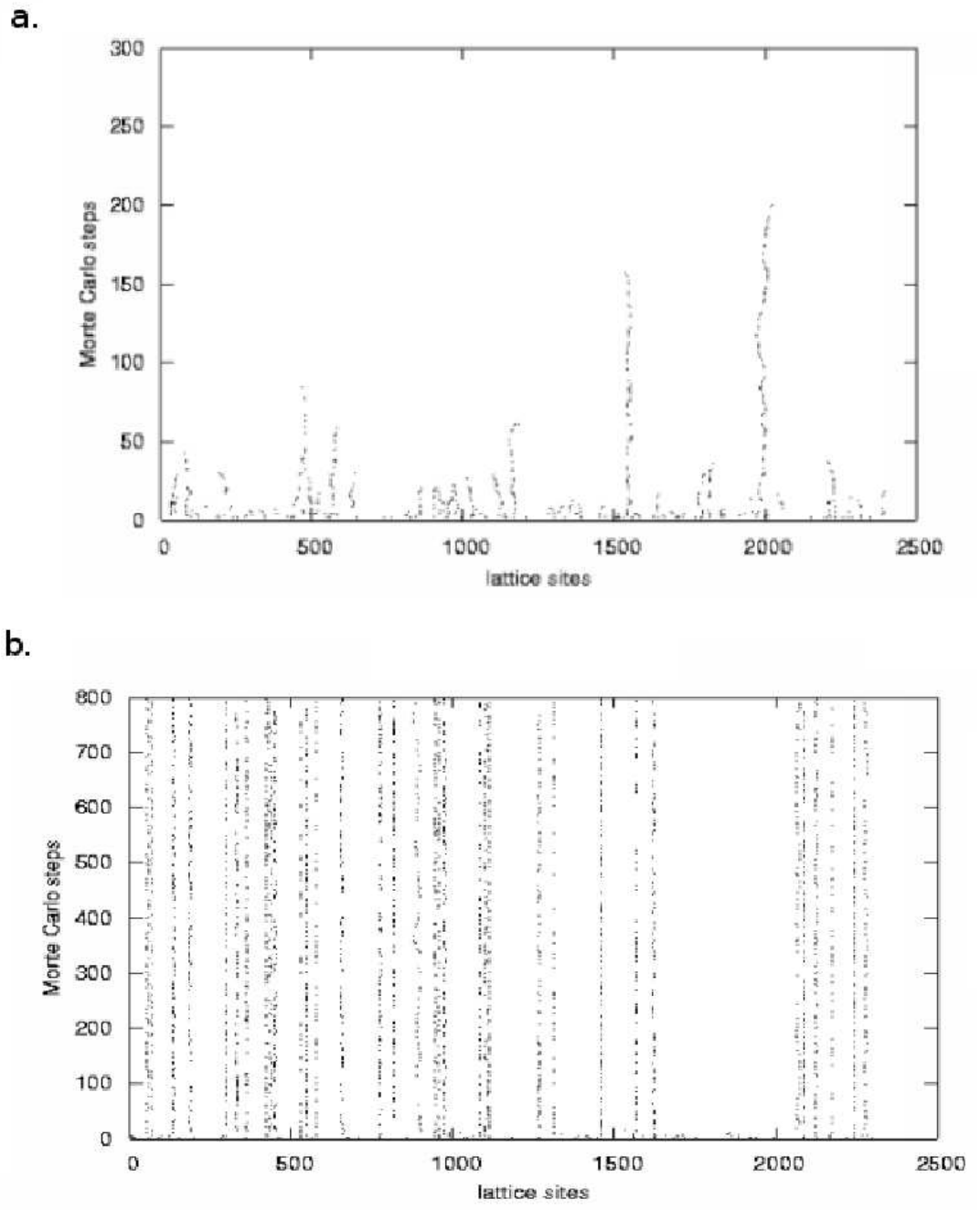

Figure 4.3: The final state reached by the system is dependent on the initial configuration. The system was quenched to the 6H phase ($J_1 = 0.9, J_2 = 0.0, J_3 = -0.6$) from **a**. 3C phase,$T = 0$ and **b**. random configuration. In the first case the system goes to a 'locked' state but in the second case there are 'active' spins even after large number of Monte Carlo steps. Here a black dot denotes that the spin at that site is active, i.e., it flips at that Monte Carlo step. The system size was taken to be 2400. Here the Monte Carlo steps shown is steps per site.

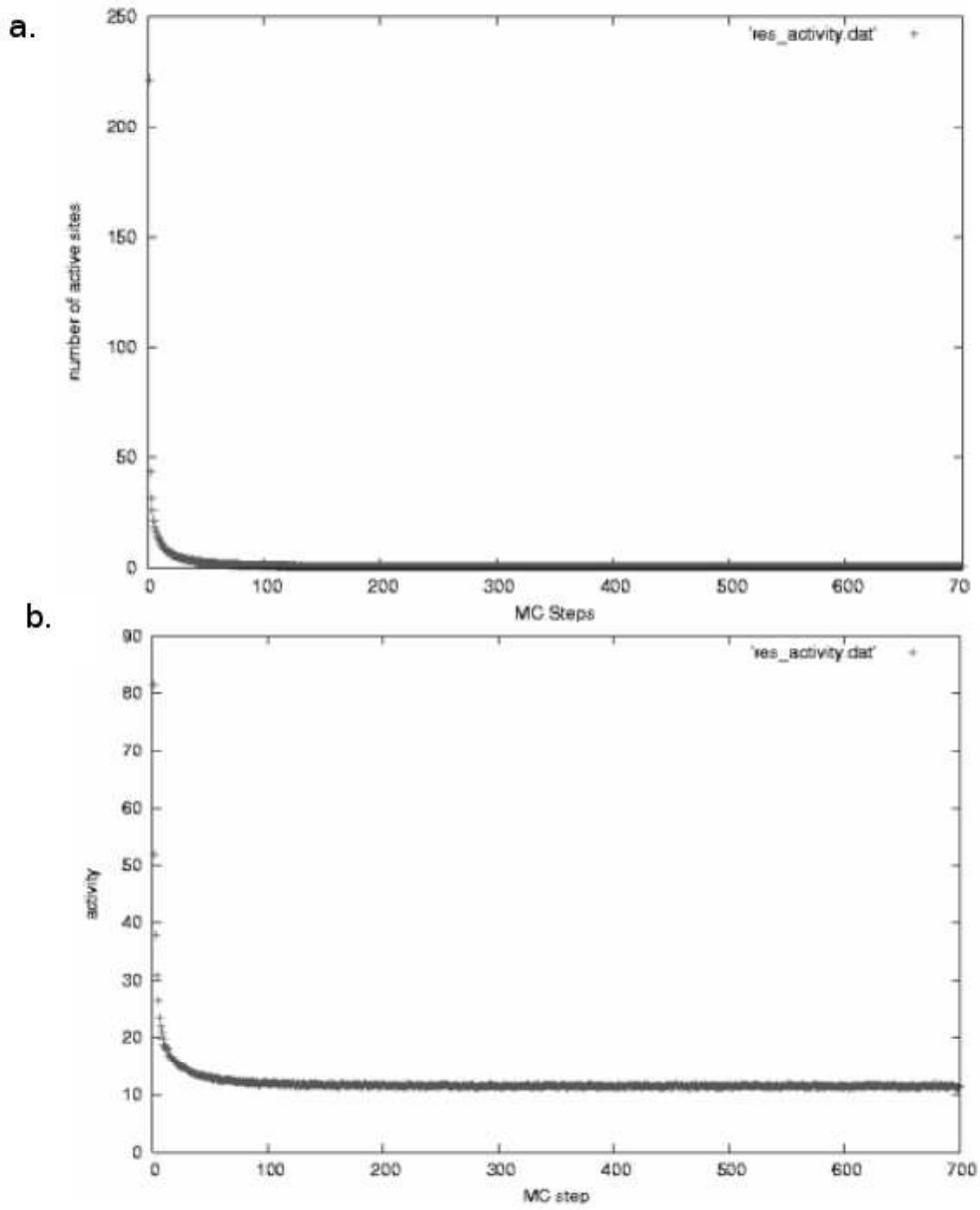

Figure 4.4: Number of site that are active at different Monte Carlo time steps when quenched to 6H phase. System size=480, $J_1 = 0.9, J_2 = 0.0, J_3 = -0.6$, The initial configuration is **a**. all 'up', **b**. random. The data were averaged over histories. Number of active sites after large number of Monte Carlo steps are proportional to the system size. Here the Monte Carlo steps shown is steps per site.

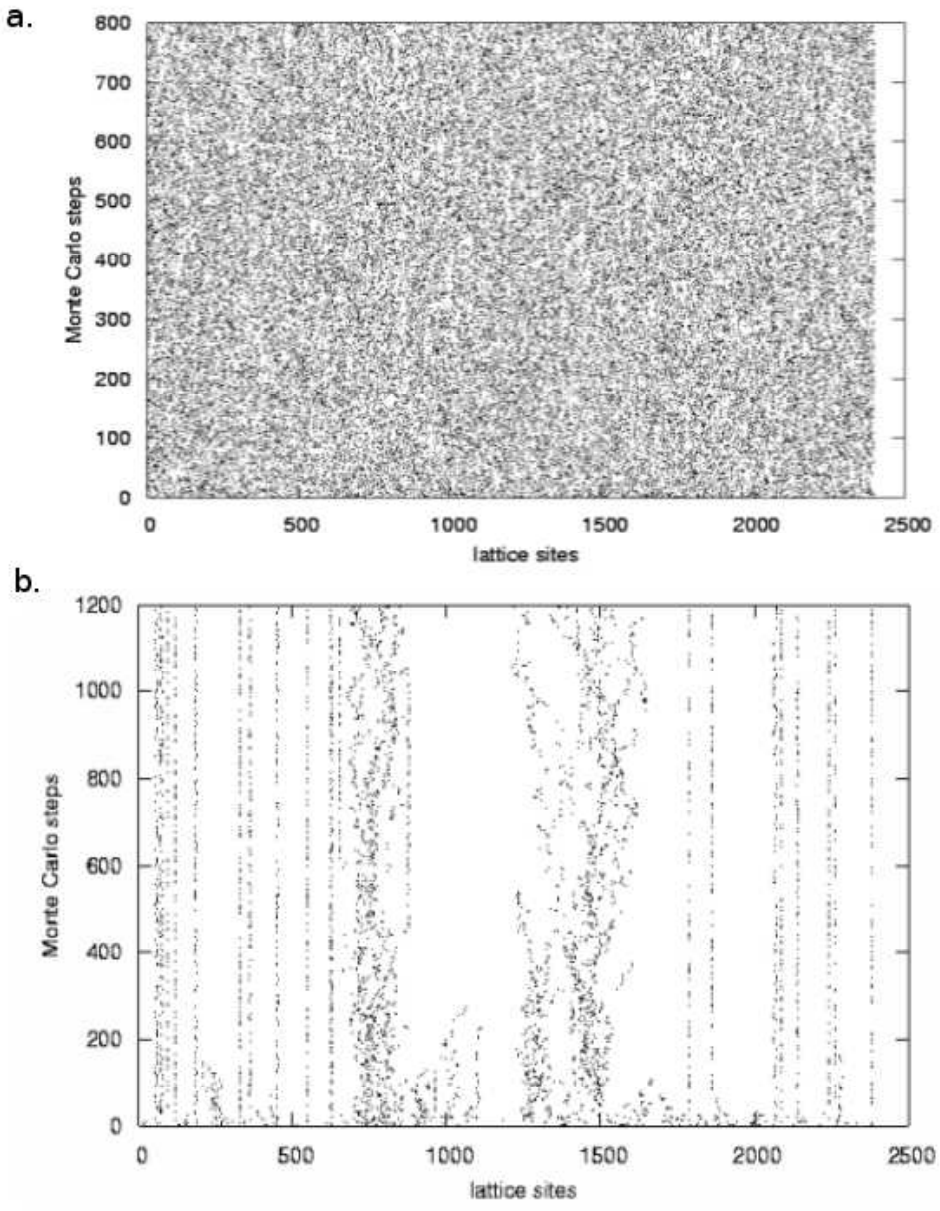

Figure 4.5: The system of size 2400 was quenched to the 3C-6H degeneracy line. The final state was again found to depend on the initial states: **a**. 3C state, all 'up' spins and **b**. random configuration. When the system starts from all 'up' it does not go to a 'locked' state but for the other case we observe patches of 'active' and 'locked' sites. 'Black' dots represent activity at that Monte Carlo step. Here the Monte Carlo steps shown is steps per site.

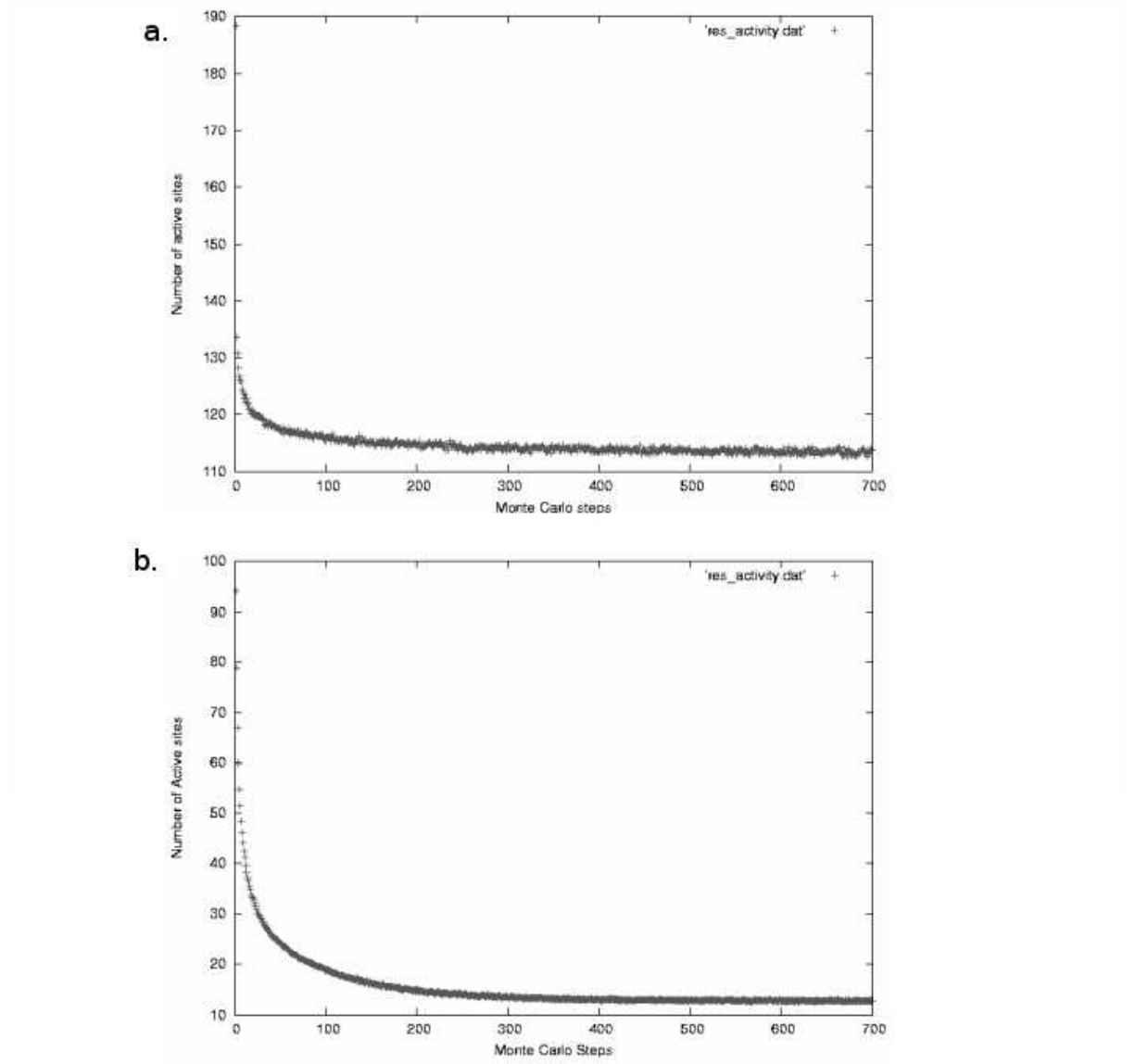

Figure 4.6: Number of site that are active at different Monte Carlo time steps when quenched to 3C-6H multiphase line. System size=480,$J_1 = 0.9, J_2 = 0.0, J_3 = -0.3$, The initial configuration is **a**. all 'up', **b**. random. The data were averaged over histories. Here the Monte Carlo steps shown is steps per site.

References

[1] S. Aubry, *Solitons and Condensed Matter Physics, ed A R Bishop and T Sneider*. Berlin: Springer Verlag, (1979). 3, 8

[2] P. Bak, *Commensurate phases, incommensurate phases and the devil's staircase*, *Rep. Prog. Phys.* **45** (1982) 587–629. 3, 8, 9, 11, 12

[3] P. Bak and J. von Boehm, *Ising model with solitons, phasons, and "the devil's staircase"*, *Phys. Rev. B* **2** ((1980)), no. 11 5297–5309. 3, 17, 19, 29, 30, 31, 33, 34

[4] M. E. Fisher and W. Selke *Phys. Rev. Lett.* **44** ((1980)) 1502. 4, 13, 21

[5] M. E. Fisher and W. Selke *Phil. Trans. R. Soc. Lond. A* **302** ((1981)), no. 146 1–44. 4, 16, 21, 22

[6] A. R. Verma and P. Krishna, *Polymorphism and Polytypism in crystals*. John Wiley and Sons, Inc., New York, (1966). 5, 36, 37

[7] D. Das and M. Barma, *Polytype kinetics and quenching of spin chains with competing interactions using trimer-flip dynamics*, *Physica A* **270** ((1999)) 245–252. 5

[8] C. Cheng, R. J. Needs, and V. Heine, *Inter-layer interactions and the origin of sic polytypes*, *J. Phys. C: Solid State Phys.* **21** (1988) 1049–1063. 5, 6, 38

[9] Y. I. Frenkel and T. Kontorowa *Zh. Eksp. Teor. Fiz.* **8** ((1938)) 1340. 8

[10] F. C. Frank and V. der Merwe *Proc. R. Soc.* **198** ((1949)) 205,216. 8

[11] G. Theodorou and T. M. Rice *Phys. Rev. B* **18** ((1978)) 2840. 8

[12] P. Bak and V. J. Emery *Phys. Rev. Lett.* **36** ((1976)) 978. 11, 32

[13] D. E. Moncton et al, *Synchrotron x-ray study of the commensurate-incommensurate transition on monolayer krypton on graphite*, *Phys. rev. Lett* **46** ((1981)), no. 23 1533–1536. 12

[14] R. J. Elliot *Phys. Rev.* **124** ((1961)) 346. 13

[15] G. D. Price and J. Yeomans *Acta Cryst.* **B40** ((1984)) 448–454. 14, 15

[16] R. Moessner *Can. J. Phys* **79** ((2001)) 1283. 15

[17] M. Droz and M. D. Coutinho-Filho *AIP Conf. Proc.* **29** ((1976)) 465. 17

[18] D. A. Huse and M. E. Fisher, *The decoupling point of the axial nearest neighbour ising model and marginal crossover*, *J. Phys. C: Solid State Physics* **15** ((1982)) L585–L595. 17

[19] J. M. Yeomans, *Splitting the multiphase point*, *arXiv:cond mat/9506129 v1* ((1995)). 26

[20] M. E. Fisher and A. M. Szpilka, *Domain-wall interactions I general features and phase diagram for spatially modulated phases*, *Phys. Rev. B* **36** ((1987)) 644. 26

[21] M. E. Fisher and A. M. Szpilka, *Domain-wall interactions II general features and phase diagram for spatially modulated phases*, *Phys. Rev. B* **36** ((1987)) 5343. 26

[22] W. L. McMillan *Phys. Rev. B* **14** ((1976)) 1496. 32

[23] W. L. McMillan *Phys. Rev. B* **16** ((1977)) 4655. 32

[24] W. Selke *Physics Reports* **170, No.4** ((1988)) 213–264. 35

[25] M. Yoshida, *Pressure-induced phase transition in sic*, *Phys. Rev. B* **48** ((1993)) 10587–10590. 36

[26] S. Sugiyama and M. Togaya *J. Am. Ceram. Soc.* **84[12]** ((2001)) 3013–3016. 36

[27] H. Baumhauer *Z. Krist* **50** ((1912)) 33–39. 37

[28] H. Baumhauer *Z. Krist* **55** ((1915)) 249–259. 37

[29] L.S.Ramsdell *Am. Mineralogist* **32** ((1947)) 64–82. 37

[30] G.S.Zhdanov *Compt. Rend. Acad. Sci. URSS* **48** ((1945)) 43. 37

[31] Adamsky and K.M.Merz *Z Krist* **111** ((1959)) 350–361. 37

[32] G. Honjo, S. Miyake, and T. Tomita *Acta Cryst* **3** ((1950)) 396–397. 37

[33] A.W.Hull *Phys Rev 13* ((1919)) 292–295. 38

[34] A.W.Hull *Phys Rev 15* ((1920)) 545–546. 38

[35] S.Madrix *Phys. Rev. B* **33** ((1986)) 8677–8684. 38

[36] B.K.Tiwari and O.N.Srivastava *J. Cryst Growth* **55** ((1981)) 395–397. 38

[37] R. M. Mitchell et al *J. Cryst Growth* **57** ((1982)) 273–279. 38

[38] S.K.Chaudhary and G.C.Trigunayat *J. Cryst Growth* **57** ((1982)) 558–562. 38

[39] F. C. Frank *Philos. Mag.* **42** ((1951)) 1014–1021. 38

[40] N. W. Jepps and T. F. Page *J. Cryst. Growth Charact.* **7** ((1983)) 259–308. 38

[41] G. D. Price *Phys. Chem. Miner.* **10** ((1983)) 77–83. 38

[42] V. K. Kabra and D. Pandey *Phys. Rev. Lett.* **61** ((1988)) 1493–1496. 39